

UNCLASSIFIED

AD NUMBER

ADB007306

LIMITATION CHANGES

TO:

Approved for public release; distribution is unlimited.

FROM:

Distribution authorized to U.S. Gov't. agencies only; Test and Evaluation; OCT 1975. Other requests shall be referred to Naval Weapons Center, China Lake, CA.

AUTHORITY

NWC ltr 13 Mar 1978

THIS PAGE IS UNCLASSIFIED

THIS REPORT HAS BEEN DELIMITED
AND CLEARED FOR PUBLIC RELEASE
UNDER DOD DIRECTIVE 5200.20 AND
NO RESTRICTIONS ARE IMPOSED UPON
ITS USE AND DISCLOSURE.

DISTRIBUTION STATEMENT A

APPROVED FOR PUBLIC RELEASE;
DISTRIBUTION UNLIMITED.

L

12

AD B007306

THIN - A Computer Program for Analyzing the Axisymmetric Behavior of Thin Spherical Shells

by
Harry E. Williams
Propulsion Development Department

OCTOBER 1975

DDC
RECEIVED
NOV 3 1975
C

Distribution limited to U.S. Government agencies only; test and evaluation; 29 August 1975. Other requests for this document must be referred to the Naval Weapons Center.

AD No. _____
DDC FILE COPY

Naval Weapons Center

CHINA LAKE, CALIFORNIA 93555



Naval Weapons Center

AN ACTIVITY OF THE NAVAL MATERIAL COMMAND

R. G. Freeman, III, RAdm., USN Commander

G. L. Hollingsworth Technical Director

FOREWORD

This report describes one phase of a program which began in July 1973 and continued through June 1975 to develop a combined aero-thermal-stress computer code capable of efficiently predicting temperature and stress distributions in axisymmetric seeker domes. The goal of the program was the determination of worst case design/flight conditions for tactical missile seeker domes. The program was accomplished through the Structures Branch, Code 4571, Naval Weapons Center, and supported by the Naval Air Systems Command, Code 320-B under AirTask A320-3200/008B/5F32-320-206.

This report is released for information primarily at the working level and does not necessarily reflect the views of NWC. The report has been reviewed for technical accuracy by Dennis L. Potts.

Released by
R. W. FEIST, *Head*
Propulsion Systems Division
18 July 1975

Under authority of
G. W. LEONARD, *Head*
Propulsion Development Department

NWC Technical Publication 5785

Published by
Collation
First printing

Technical Information Department
Cover, 25 leaves
65 unnumbered copies

ACCESSION FOR
NTIS
DOC
UNANNOUNCED
JUSTIFICATION

BY DISTRIBUTION AVAILABLE TO
DIS. 2 APR 1976

B

UNCLASSIFIED

SECURITY CLASSIFICATION OF THIS PAGE (When Date Entered)

UNCLASSIFIED

REPORT DOCUMENTATION PAGE		READ INSTRUCTIONS BEFORE COMPLETING FORM
1. REPORT NUMBER 14 NWC-TP-5785	2. GOVT ACCESSION NO.	3. RECIPIENT'S CATALOG NUMBER 9
4. TITLE (and Subtitle) 6 THIN - A COMPUTER PROGRAM FOR ANALYZING THE AXISYMMETRIC BEHAVIOR OF THIN SPHERICAL SHELLS.		5. TYPE OF REPORT & PERIOD COVERED Summary <i>rept.</i> Jul. 1973 - Jun. 1975
7. AUTHOR(s) 10 Harry E. Williams		6. PERFORMING ORG. REPORT NUMBER
	12 49 p.	8. CONTRACT OR GRANT NUMBER(s)
9. PERFORMING ORGANIZATION NAME AND ADDRESS Naval Weapons Center China Lake, CA 93555		10. PROGRAM ELEMENT, PROJECT, TASK AREA & WORK UNIT NUMBERS 16 ATTASK A320-3200/008B/5F32-320-206 320 206
11. CONTROLLING OFFICE NAME AND ADDRESS Naval Air Systems Command Washington, DC 20360	11	12. REPORT DATE Oct. 1975
		13. NUMBER OF PAGES 48
14. MONITORING AGENCY NAME & ADDRESS (if different from Controlling Office)		15. SECURITY CLASS. (of this report) Unclassified
		15a. DECLASSIFICATION/DOWNGRADING SCHEDULE
16. DISTRIBUTION STATEMENT (of this Report) Distribution limited to U.S. Government agencies only; test and evaluation; 29 August 1975. Other requests for this document must be referred to the Naval Weapons Center.		
17. DISTRIBUTION STATEMENT (of the abstract entered in Block 20, if different from Report)		
18. SUPPLEMENTARY NOTES		
19. KEY WORDS (Continue on reverse side if necessary and identify by block number) Thin Spherical Shells Thermal Stress Finite Differences Dynamics Dynamic Relaxation Thermal Elastic Linearly Elastic Computer Solution Small Deflection		
20. ABSTRACT (Continue on reverse side if necessary and identify by block number) See reverse side of this form.		


403 019

MX

(U) *THIN - A Computer Program for Analyzing the Axisymmetric Behavior of Thin Spherical Shells*, by Harry E. Williams. China Lake, Calif., NWC, October 1975, 48 pp. (NWC TP 5785.)

(U) The computer program THIN obtains the solution of the equations of equilibrium governing the small deflections of thin spherical shells using an algorithm called "Dynamic Relaxation." It is assumed that the material properties of the shell are constant and that the shell is closed at the apex. The conditions at the outer edge can be chosen to be either clamped, simply-supported or supported on a transverse roller-skate.

(U) This report describes the input/output requirements of the program, the behavior of the "Dynamic Relaxation" algorithm and estimates the accuracy of the program by comparing numerical results obtained using THIN with either exact analytical solutions or analytical solutions where accuracy can be assessed.



CONTENTS

Introduction	3
Input Requirements and the Output of THIN	6
Analysis of THIN	19
The Use of THIN - Examples	12
Appendixes	
A. The Governing Equations	29
B. Critical Damping Factor	31
C. The Temperature Integrals	33
D. The Stress Distribution	35
E. Asymptotic Solution for a Thin Shell	37
F. Program Listing	45

NOMENCLATURE USED IN THIN

The following nomenclature is used in THIN in addition to the input/output terms which are described in the report.

THIN	Appendix A
CHIB	\bar{X}
EPPB	$\bar{\epsilon}_\phi$
EPTB	$\bar{\epsilon}_\theta$
FKPB	$\bar{\kappa}_\phi$
FKTB	$\bar{\kappa}_\theta$
FMPB	\bar{M}_ϕ
FMTB	\bar{M}_θ
FNPB	\bar{N}_ϕ
FNTB	\bar{N}_θ
QB	\bar{Q}
SIGB	$\sigma_{\phi\phi}/E$
THB	$\bar{\Theta}$
TMB	\bar{T}_m
VB	\bar{v}
VBD	$\frac{\partial \bar{v}}{\partial \tau}$
WB	\bar{w}
WBD	$\frac{\partial \bar{w}}{\partial \tau}$

INTRODUCTION

THIN is a special purpose program which can be used to obtain the stresses and displacements in a spherical shell acted upon by an axisymmetric distribution of normal and/or tangential pressure, and heated arbitrarily through the shell thickness to a prescribed axisymmetric temperature distribution. It is assumed that the shell is closed at the apex, and supported along the edge (see Figure 1) such that the edge is either:

1. Clamped-displacements (v , w), rotation (X) all vanish, or
2. Simply-supported-displacements (v , w), meridional bending moment (M_ϕ) all vanish. or
3. Roller-skate supported-tangential displacement (v), transverse shear (Q_ϕ) and meridional bending moment (M_ϕ) all vanish.

Further, it is assumed that the material is linearly elastic, and characterized by material parameters (E , ν , α) which do not depend on the temperature. (This feature of the program could readily be included, but was omitted here to limit the length of the program.)

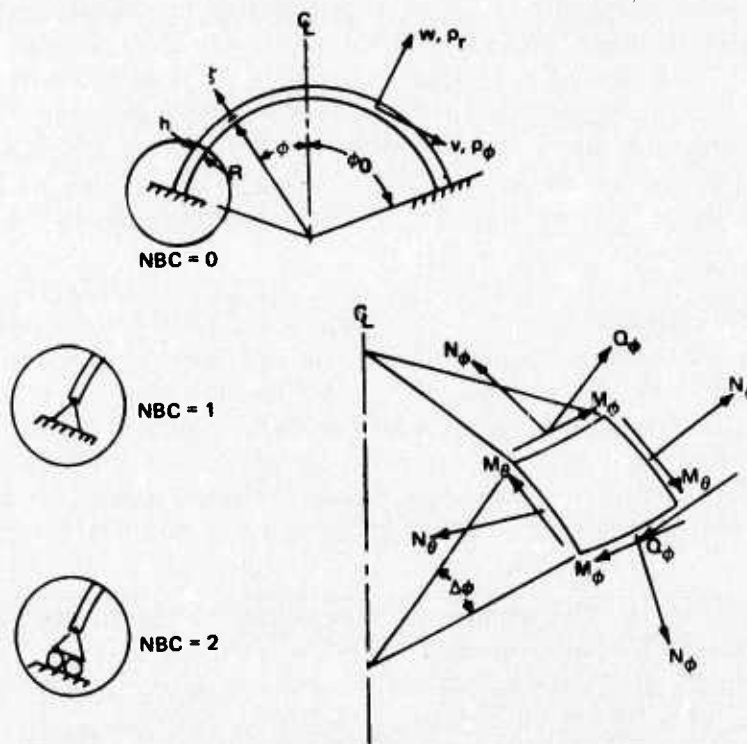


FIGURE 1. Notation and Boundary Conditions.

THIN obtains solutions of the axisymmetric, thin shell equations appropriate to spherical shells (see Appendix A). It is based on an algorithm developed by Otter¹ and termed by him "Dynamic Relaxation (D.R.)". In essence, the static problem, which is governed by a system of ordinary differential equations and associated boundary conditions, is replaced by a dynamic problem governed by a system of partial differential equations and the same boundary conditions. The success of the method depends on the fact that the dynamic problem is relatively easier to solve numerically than is the static problem.

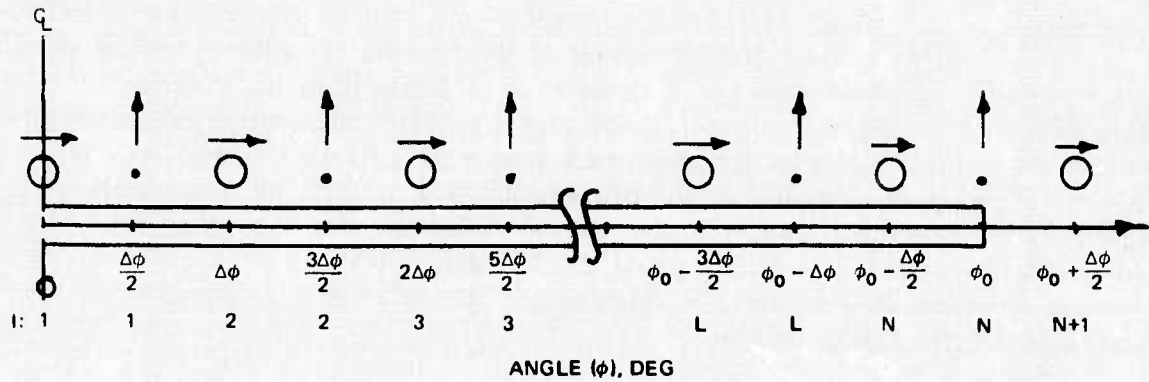
The associated dynamic problem is governed by the equations of motion appropriate to spherical shells in which are included hypothetical viscous damping terms. If the damping parameters (K_r , K_ϕ) have been chosen properly, the solution of the equations of motion should decay to the required solution of the equations of equilibrium in about one to two periods of the lowest mode of vibration of the shell corresponding to the particular type of support. (Note that rigid body motion must be constrained in order to conveniently identify convergence of the dynamic solution to the required equilibrium solution.) The use of D.R. generally requires that the program be first run in an *experimental* mode with zero damping in order to identify the period of the lowest mode of vibration. This phase could be omitted if this information could conveniently be obtained elsewhere, i.e., analytically. However, it is often more easily obtained *experimentally*. The required solution is obtained by running the program again in the damped mode, and is the limiting form of the time varying solution as time becomes large (about 1 1/2 periods of the lowest mode of free vibration). In a qualitative way, the shell is first impulsively loaded and allowed to vibrate freely (without damping) for a length of time adequate to observe some semblance of periodic motion. This *experiment* is then followed by a trial run in which the shell is again impulsively loaded, but now damping is included and the motion is observed for a length of time adequate for the kinetic energy to be dissipated. For further details of D.R., the reader is referred to Rushton.² In what follows, the theory will be implemented insofar as it applies to the particular problem at hand.

THIN operates with the thin shell equations made dimensionless with the introduction of a suitable time scale and appropriate dependent variables. These equations (Appendix A) are then written in finite difference form using the interlacing network in both space (the meridional opening angle- ϕ) and time that was suggested by Gilles³ for improving the accuracy of the finite difference representation of derivatives. Thus, it is observed from Figures 2 and 3 that all the dependent variables are not defined at the same point in either space or time. In particular, the transverse

¹ Otter, J. R. H. "Computations for Pre-stressed Concrete Pressure Vessels Using Dynamic Relaxation," Nuclear Structural Engineering, 1 (1965) Amsterdam, pp. 61-75.

² Rushton, K. R. "Dynamic-Relaxation Solutions of Elastic-Plate Problems," JOURNAL OF STRAIN ANALYSIS, Vol. 3, 1 (1968), pp. 23-32.

³ Gilles, D. C., "The Use of Interlacing Nets for the Application of Relaxation Methods to Problems Involving Two Dependent Variables," PROC ROYAL SOC. A (1948), 193, pp. 407-433.



NOMENCLATURE

SYMBOL	QUANTITIES EVALUATED
•	$\bar{\epsilon}_\phi, \epsilon_\theta; \bar{\kappa}_\phi, \bar{\kappa}_\theta$
↑	$\bar{N}_\phi, \bar{N}_\theta; \bar{M}_\phi, \bar{M}_\theta; T$
○	\bar{w}, \bar{q}
→	\bar{v}, \bar{p}

FIGURE 2. Spacial Format.

M	t	QUANTITIES EVALUATED
3	$2\Delta t$	DISPLACEMENTS, ACCELERATIONS
3	$\frac{3\Delta t}{2}$	VELOCITIES
2	Δt	DISPLACEMENTS, ACCELERATIONS
2	$\frac{\Delta t}{2}$	VELOCITIES
1	0	DISPLACEMENTS, ACCELERATIONS
1	$-\frac{\Delta t}{2}$	VELOCITIES

FIGURE 3. Temporal Format.

displacement (w) is defined on 1/2-integral multiple values of the meridional coordinate interval ($\Delta\phi$) and on integral multiple values of the temporal coordinate interval (Δt). Note that the transverse velocity is defined on 1/2-integral multiple values of the temporal coordinate interval. In comparison, the tangential displacement (v) is defined on integral multiple values of the meridional coordinate interval, and also on integral multiple values of the temporal coordinate spacing. In this way, the representation of derivatives or differences always involve central differences. On the other hand, not having quantities defined at points where the boundary conditions are imposed can be awkward. However, this difficulty is overcome by the use of *dummy* points which are located outside the regular interval.

A typical solution is generated by first assuming the shell to be quiescent (displacement, velocity all zero) and loaded by the given external load and/or heated to the prescribed temperature distribution. As this condition can exist only if there is a non-zero value for the acceleration, there is motion away from the initial configuration which can be computed and continued in a step-wise manner until either the period of the fundamental mode of vibration is identified, or satisfactory convergence to the equilibrium solution is achieved.

In the sections which follow, the input requirements and the output are described. There then follows a description of the program with details on how the parameters of the program are chosen. Examples are presented of typical dynamic response and results given for both constant transverse pressure loading and uniform temperature rise. Finally, the accuracy of the program is assessed by comparing the results of THIN with analytical predictions—again for the case of constant transverse pressure.

INPUT REQUIREMENTS AND THE OUTPUT OF THIN

In order to use THIN, the following must be provided.

Material Data

ν (=PR)	Poisson's ratio (dimensionless)
α (=ALFA)	Coefficient of thermal expansion ($1/^\circ\text{F}$)

(Young's Modulus, E , is not required as the output stresses are presented in dimensionless form, i.e., $\bar{\sigma}_{\phi\phi} = \sigma_{\phi\phi}/E$).

Geometric Data

ϕ_0 (=PO)	Meridional opening angle at which boundary conditions are prescribed (dimensionless, radians)
\bar{h} (=HB)	Thickness ratio (h/R) (dimensionless)

NWC TP 5785

(The thickness, h , is not required as the output displacements are expressed in dimensionless form, i.e., $w = \bar{w}/h$.)

N A measure of the number of segments (see Figure 2) into which the meridional length of the shell is divided ($N = \frac{1}{2} + \frac{\phi_0}{\Delta\phi}$) (integer)

Control Data

K_r (=CKR),
 K_ϕ (=CKP) Damping factors (dimensionless) (See Appendix B)

NBC An index which determines (see Figure 1) the boundary conditions (integer)

NV An index which determines the meridional station at which the tangential displacement is to be studied during the *experimental* phase of operation (integer)

MMAX An index which determines the number of iterations through which THIN cycles in either phase of operation (integer)

IDEC An index which determines the interval between iterations whose typical displacements are printed out during the *experimental* phase of operation (integer)

IPRNT An index which determines the output required (integer)
 IPRNT=0 Typical displacements every IDEC number of iterations only
 IPRNT=1 Typical displacements every IDEC number of iterations, plus the solution after MMAX iterations expressed in dimensionless variables
 IPRNT=2 The solution after MMAX iterations only

Mechanical Loading and Temperature Distribution Data

\bar{p} (=PB) Dimensionless tangential pressure distribution. Must be prescribed at N-meridional stations (see Figure 2) even though the apex value is never used, and, from symmetry, must be zero (subscripted variable)

\bar{q} (=QPB) Dimensionless transverse pressure distribution. Must be prescribed (see Figure 2) at N-meridional stations even though the edge value is only used for the roller-skate support condition (subscripted variable)

T_{REF} (=TREF) Reference temperature at which the stresses, strains are assumed to vanish ($^{\circ}R$)

NWC TP 5785

T (=IMP) Temperature distribution. Temperature must be prescribed (see Figure 4 and Appendix C) at 5 points through the thickness of the shell, at N-meridional stations (subscripted variable, °R)

These data are read into the program from cards provided by the user. The first card contains

$$\phi_0 \quad \bar{h} \quad \nu \quad K_r \quad K_\phi$$

and is read in the open format. The second card contains

$$T_{REF} \quad \alpha$$

and is read in the open format. The third card contains

$$NBC \quad N \quad NV \quad MMAX \quad IDEC \quad IPRNT$$

and is read in the 6110 format. There then follows N-cards with the number pairs:

$$\bar{q} \quad \bar{p}$$

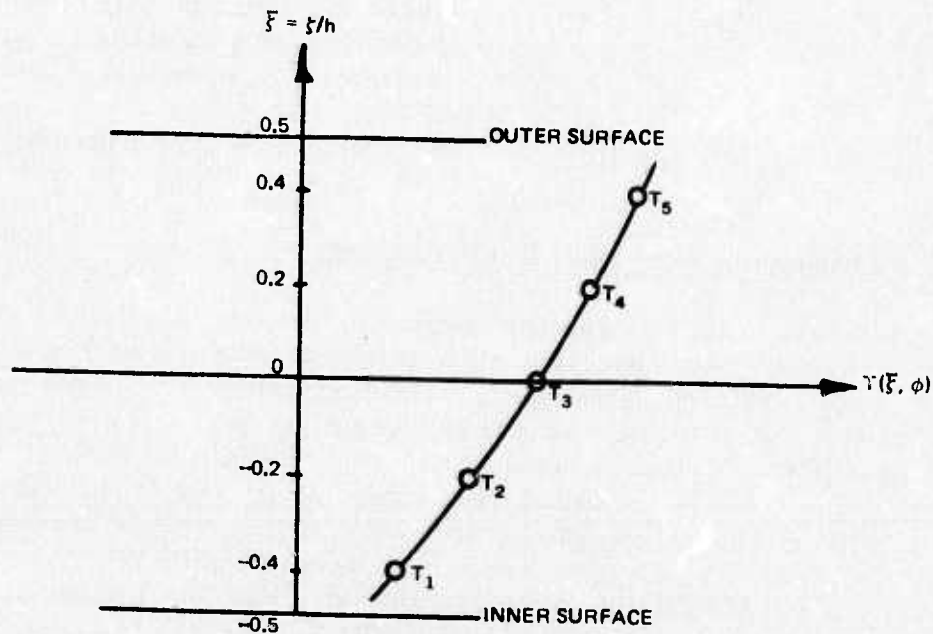


FIGURE 4. Typical Temperature Distribution.

for each of N-meridional stations. These cards are read in the open format. Note (see Figure 2) that the values of \bar{p} , \bar{q} are not measured at the same point in space due to the use of the interlacing network. Finally, there follows N-cards with the temperature distribution (see Figure 4)

$$T_1 \quad T_2 \quad T_3 \quad T_4 \quad T_5$$

through the thickness of the shell for each of N-meridional stations. These cards are also read in the open format.

In its present form, the output of THIN always includes a record of the temperature and the applied pressure distribution, and also the temperature integrals \bar{T}_m , $\bar{\Theta}$ computed according to Appendix C. The output can also include (1) the time response of both the transverse displacement of the meridional station nearest the apex ($I=1$) and the tangential displacement of the meridional station $I=Nv$, and (2) the solution after MMAX iterations expressed in dimensionless variables. The index IPRNT is used to identify the option. The displacements at $I=1(\bar{w})$, $I=Nv(\bar{v})$ have been chosen as they represent very nearly the maximum displacements expected in the lowest mode of vibration. The index NV is taken somewhat greater than $N/2$ as it has been observed that the tangential displacement reaches a peak in this neighborhood. The time response is printed out so that the user can either estimate the period of the lowest mode of vibration or determine whether satisfactory convergence to the static solution has been achieved. The solution includes the meridional distribution of the dimensionless displacements and stress resultants, and the complete (meridional plus transverse) distribution of the dimensionless meridional normal stress ($\bar{\sigma}_{\phi\phi} = \sigma_{\phi\phi}/E$). This stress component is computed according to the method outlined in Appendix D, and is displayed as it is generally the critical stress from a maximum normal stress point of view.

ANALYSIS OF THIN

The form of the thin shell equations used in THIN is that given by Parkus and Flugge.⁴ This form was chosen as it was considered more generally accessible than other forms. The equations and their dimensionless forms are presented in Appendix A. THIN actually operates with the finite difference form of these equations using the interlacing network illustrated in Figure 2.

The D.R. algorithm can be illustrated by studying the equations which govern the transverse displacement (w). At the beginning of a typical iteration, the displacements $\bar{w}(I)$ and the velocities $\frac{\partial \bar{w}}{\partial \tau}(I)$ are known at all points in space ($1 \leq I \leq N$). It should be noted (see Figure 3) that the velocities are known at a time (corresponding

⁴ Flugge, W., *Handbook of Engineering Mechanics*, McGraw-Hill, 1962.

to the index M) which is less than the time (also corresponding to the index M) at which the displacements are known. For the first iteration (M=1), these displacements and velocities are all taken equal to zero. Before proceeding to the next iteration, the strain components $\bar{\epsilon}_\phi$, $\bar{\epsilon}_\theta$ are first computed. For example, from Appendix A, we write

$$\bar{\epsilon}_\phi(I) = \bar{w}(I) + [\bar{v}(I+1) - \bar{v}(I)]/\Delta\phi$$

In an analogous manner, the rotation \bar{X} is also computed. With the strain, rotation components now known at all points in space, the in-plane force and moment stress resultants follow directly from the constitutive equations—the temperature integrals having been computed (see Appendix C) during the data loading phase. The transverse stress resultant (\bar{Q}) is then obtained from the equation of moment equilibrium expressed in the form

$$\bar{Q}(I) = [\bar{M}_\phi(I) - \bar{M}_\phi(I-1)]/\Delta\phi + [\bar{M}_\phi(I) - \bar{M}_\theta(I) + \bar{M}_\phi(I-1) - \bar{M}_\theta(I-1)] \frac{\cot \phi}{2}$$

Note that the use of this equation is, strictly speaking, not justified in the context of a dynamic analysis. However, since the dynamical aspect used here is a computational artifice, the neglect of rotary inertia is unimportant and has no effect on the final results. With all stress resultants now known, the solution corresponding to the given displacements is complete and the stress distribution could be calculated although it is generally deferred until the last (M=M MAX) iteration. It should be noted that this solution does not in general satisfy the equation of translational equilibrium. It is precisely this fact that enables the calculation to proceed.

The displacement distribution for the next iteration (corresponding to the index M+1) is obtained from the acceleration which is computed from the translational equation of motion. This requires the definition of the acceleration expressed in terms of the velocities given by

$$\frac{\partial^2 \bar{w}}{\partial \tau^2}(M) = \left[\frac{\partial \bar{w}}{\partial \tau}(M+1) - \frac{\partial \bar{w}}{\partial \tau}(M) \right] / \Delta \tau$$

and the definition of the velocity in terms of the displacement given by

$$\frac{\partial \bar{w}}{\partial \tau}(M+1) = [\bar{w}(M+1) - \bar{w}(M)] / \Delta \tau$$

Thus, with the transverse translational equation of motion expressed in the form

$$\begin{aligned} \frac{\partial \bar{w}}{\partial \tau}(M+1)(1 + K_r/2) &= \frac{\partial \bar{w}}{\partial \tau}(M)(1 - K_r/2) + \Delta \tau \bar{q}(I) - \frac{\Delta \tau}{1 - \nu^2} (\bar{N}_\phi(I) + \bar{N}_\theta(I) + \\ &+ \frac{h^2}{12R^2} ((\bar{Q}(I+1) - \bar{Q}(I))/\Delta\phi + \frac{\cot \phi}{2} (\bar{Q}(I+1) + \bar{Q}(I)))) \end{aligned}$$

the velocities $\frac{\partial \bar{w}}{\partial \tau}(I, M+1)$ and the displacements $\bar{w}(I, M+1)$ follow directly. This completes one cycle of the D.R. algorithm save for the establishment of dependent variables at dummy points that are necessary for the satisfaction of the boundary conditions.

Following the format given on Figure 2, it is apparent that boundary conditions can be directly enforced on \bar{w} , \bar{M}_ϕ as they are defined on $\phi = \phi_0$. Alternatively, the requirement that the tangential displacement vanish at $\phi = \phi_0$ leads to the establishment of \bar{v} at the dummy point $I=N+1$ with the value

$$\bar{v}(N+1) = -\bar{v}(N)$$

Thus it is actually the average of two adjacent points which actually is required to vanish. A similar expression is used to enforce a zero condition on variables which are not defined on $\phi = \phi_0$.

The clamped boundary condition is enforced by taking

$$\bar{X}(N+1) = -\bar{X}(N)$$

It then follows that

$$\bar{\kappa}_\theta(N) = \frac{1}{2} (\bar{X}(N+1) + \bar{X}(N)) \cot \phi_0 = 0$$

$$\bar{\kappa}_\phi(N) = (\bar{X}(N+1) - \bar{X}(N))/\Delta\phi = -2\bar{X}(N)/\Delta\phi$$

which is sufficient to determine the edge values of the moment stress resultants.

The simply-supported boundary condition is enforced by taking

$$\bar{M}_\phi(N) = 0$$

This requirement is used to establish $\bar{X}(N+1)$ from the constitutive equation expressed in the form

$$\bar{M}_\phi(N) \equiv (\bar{X}(N+1) - \bar{X}(N))/\Delta\phi + \frac{\nu}{2} (\bar{X}(N+1) + \bar{X}(N)) \cot \phi_0 + (1+\nu) \alpha \Theta R/\bar{h} = 0$$

Thus, it follows that

$$\bar{X}(N+1) = (\bar{X}(N)(1 - \frac{\nu\Delta\phi}{2} \cot \phi_0) - \bar{\Theta}\Delta\phi)/(1 + \frac{\nu\Delta\phi}{2} \cot \phi_0)$$

The roller-skate boundary condition is the only option in THIN in which $w(N) \neq 0$. As the roller-skate is free to move in the transverse direction, the transverse shear must vanish leading to a dummy value for \bar{Q} given by

$$\bar{Q}(N+1) = -\bar{Q}(N)$$

With $\bar{Q}(N+1)$ now known, the transverse displacement at the edge can be computed using the transverse translational equation of motion.

THE USE OF THIN - EXAMPLES

The primary unknowns in the D.R. algorithm are the damping factors K_r , K_ϕ . In order to determine these factors (see Appendix B), the program must generally first be run in the undamped mode to estimate the lowest natural frequency. However, before this can be done, the user must choose an appropriate value for N and estimate the total number of iterations required (MMAX) to identify the period of the lowest mode of vibration.

The index N is an integer and is a measure of size of the spacial interval $\Delta\phi$. It is defined by

$$N = \frac{1}{2} + \frac{\phi_0}{\Delta\phi}$$

The choice of N is an important one, since it not only affects the accuracy of the solution, but essentially establishes the running time of the program and hence the cost. If N is large, the finite difference representation of the spacial derivatives is relatively accurate. However, the allowable time step ($\Delta\tau$) is limited by the requirements that the algorithm be numerically stable and the program must be cycled many times in order that the overall time interval be approximately 1 1/2 periods of the lowest mode. Alternatively, if N is small, the finite difference representation becomes increasingly inaccurate, but the running time is substantially reduced. In the final analysis, the choice of N can only be made on the basis of several trials with the criteria being that N is chosen to be the smallest number such that there is a negligible change in the solution corresponding to a finite increase in N .

As a general rule, the spacing along the meridian $R\Delta\phi$ should be less than the characteristic length of the shell (\sqrt{hR}). If we chose the spacing $\Delta\phi$ such that

$$R\Delta\phi = \sqrt{hR}/3$$

then, $N \approx \frac{3\phi_0}{\sqrt{h}}$, and we should obtain about ten data points in a meridional distance corresponding to three characteristic lengths.

The choice of MMAX depends on the allowable time increment $\Delta\tau$. As the equations of motion governing the spherical shell are probably of the parabolic type, we adopt the requirement established by Crandall⁵ for beams that limits the stable time step to

$$\Delta\tau \leq \frac{1}{2}\Delta\phi^2$$

Further, if we assume that the period of the lowest mode of vibration is approximately $(\tau_0 =)2\pi$, and adopt the equality in the above expression for the stable time step, a running time of a period and a half corresponds to

$$\text{MMAX} = 6\pi N^2 / \phi_0^2$$

For example, for a hemispherical shell ($\phi_0 = 90$ deg) and $N=10$, a running time of a period and a half corresponds to $\text{MMAX}=764$. With N , MMAX estimated approximately, the program may be run and improved values obtained from an examination of the solution and the time behavior.

Examples of undamped response are presented as Figures 5 through 8 for constant normal pressure loading. (The response to a constant temperature rise for the same boundary conditions and shell geometry is not shown since the curves are similar to those for constant pressure loading.) Note that as the curves have been plotted with the iteration index (M) as the abscissa (and with an iteration step size IDEC=40) the corresponding dimensionless time is different for each shell geometry and must be computed according to the relation

$$\tau = M\Delta\tau = \frac{M}{2}(\Delta\phi)^2$$

Some similarity can be seen by comparing the curves on Figures 5 and 6. It appears that the effect of the thickness parameter (\bar{h}) is greater for the tangential displacement response, as the transverse displacement response have roughly the same shape. One should hasten to add, however, that there is not complete geometric similarity between the shells as the tangential displacement was observed at $\phi \approx 52$ deg for the case $N=16$ and at $\phi \approx 42$ deg for the case $N=20$. Nevertheless, it appears that the use of τ as a time scale is justified, and that some semblance of periodic motion may be observed corresponding to a dimensionless period of about $6 < \tau < 8$. Thus, a running time (MMAX) corresponding to $\tau \approx 9$ seems to be adequate to span about 1 1/2 periods of the lowest mode of vibration for clamped boundary conditions at $\phi_0 = 90$ deg.

⁵ Crandall, S. H. *Engineering Analysis, A Survey of Numerical Procedures*, McGraw-Hill, 1956.

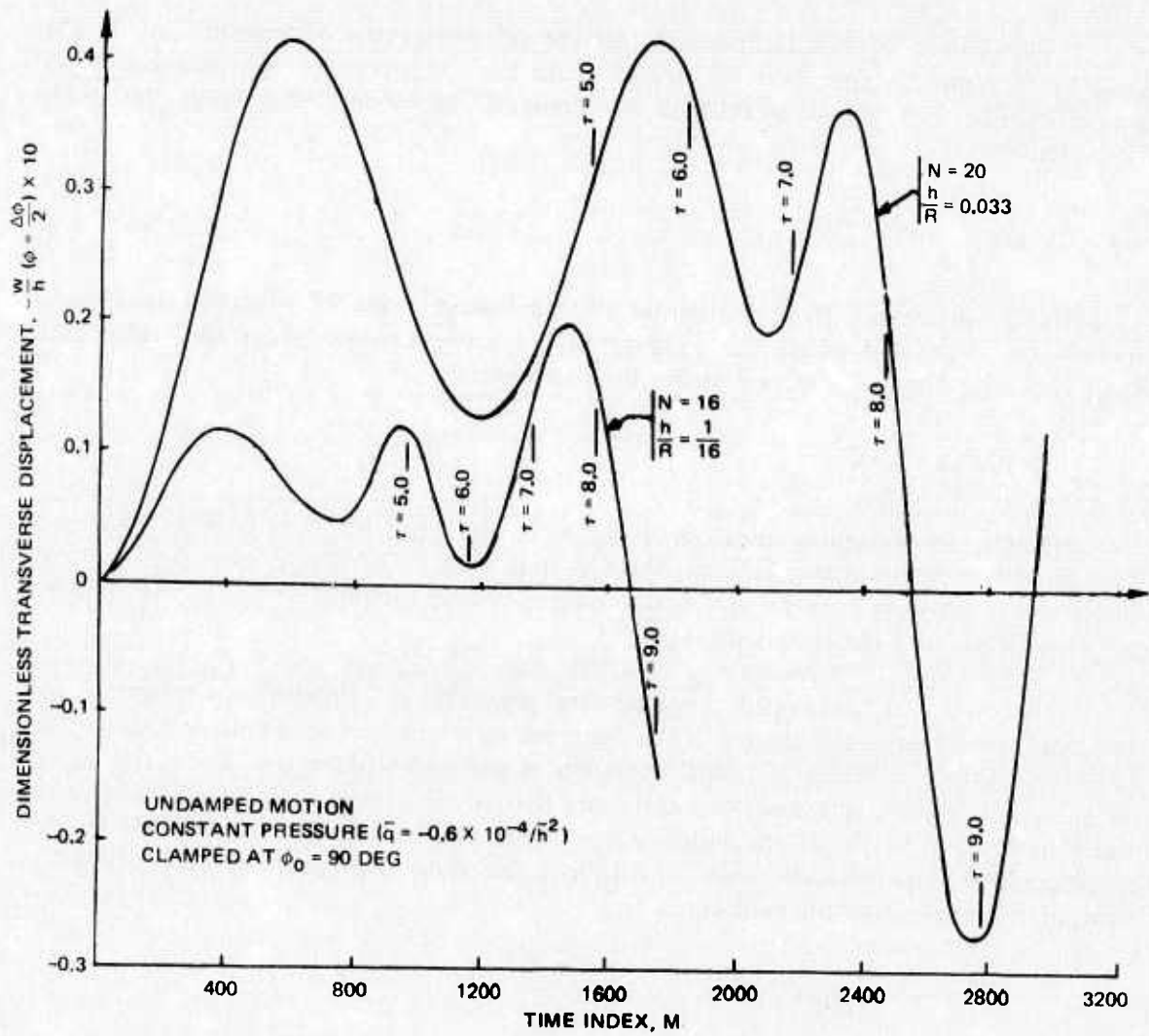


FIGURE 5. Transverse Displacement Versus Time.

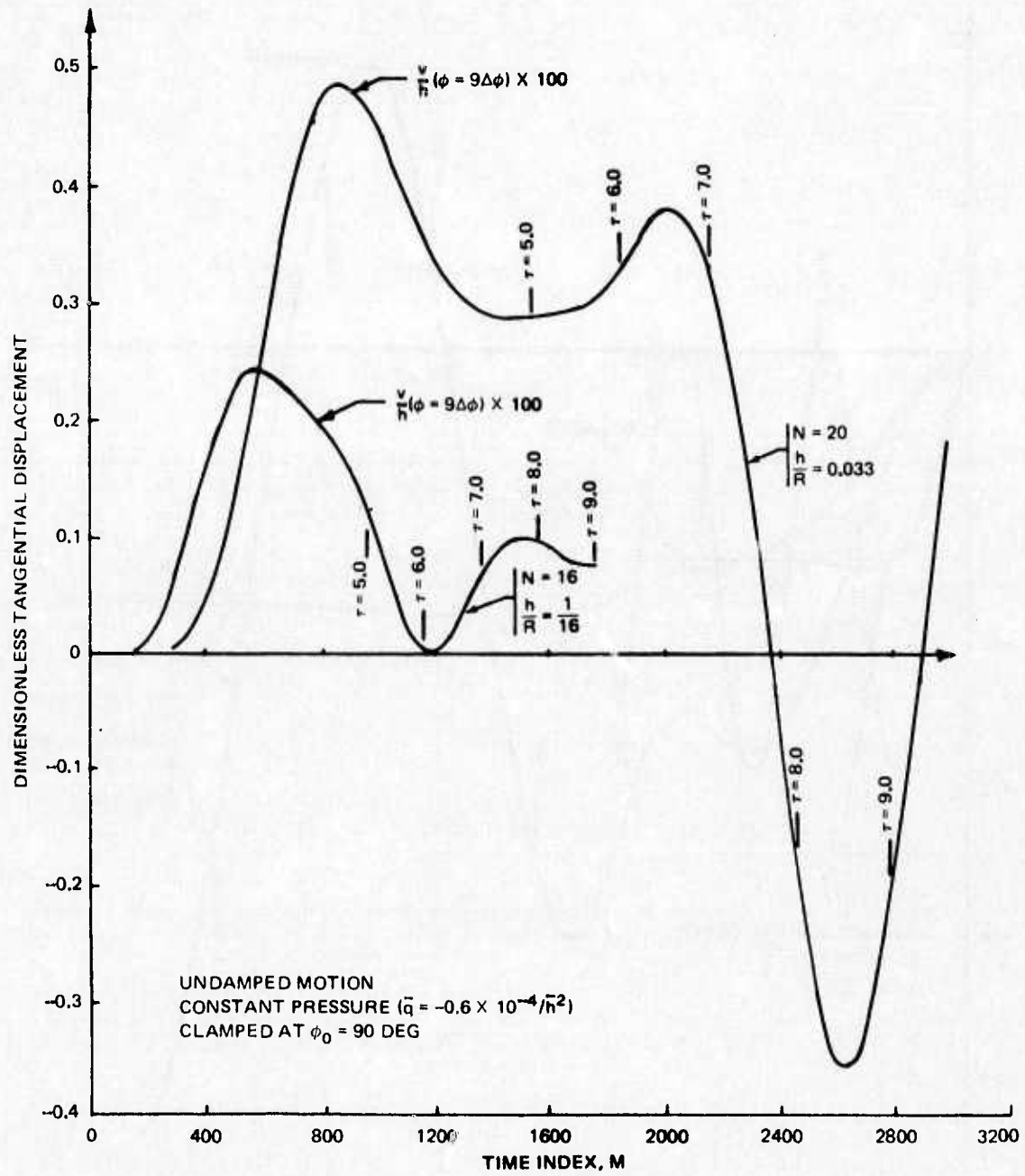


FIGURE 6. Tangential Displacement Versus Time.

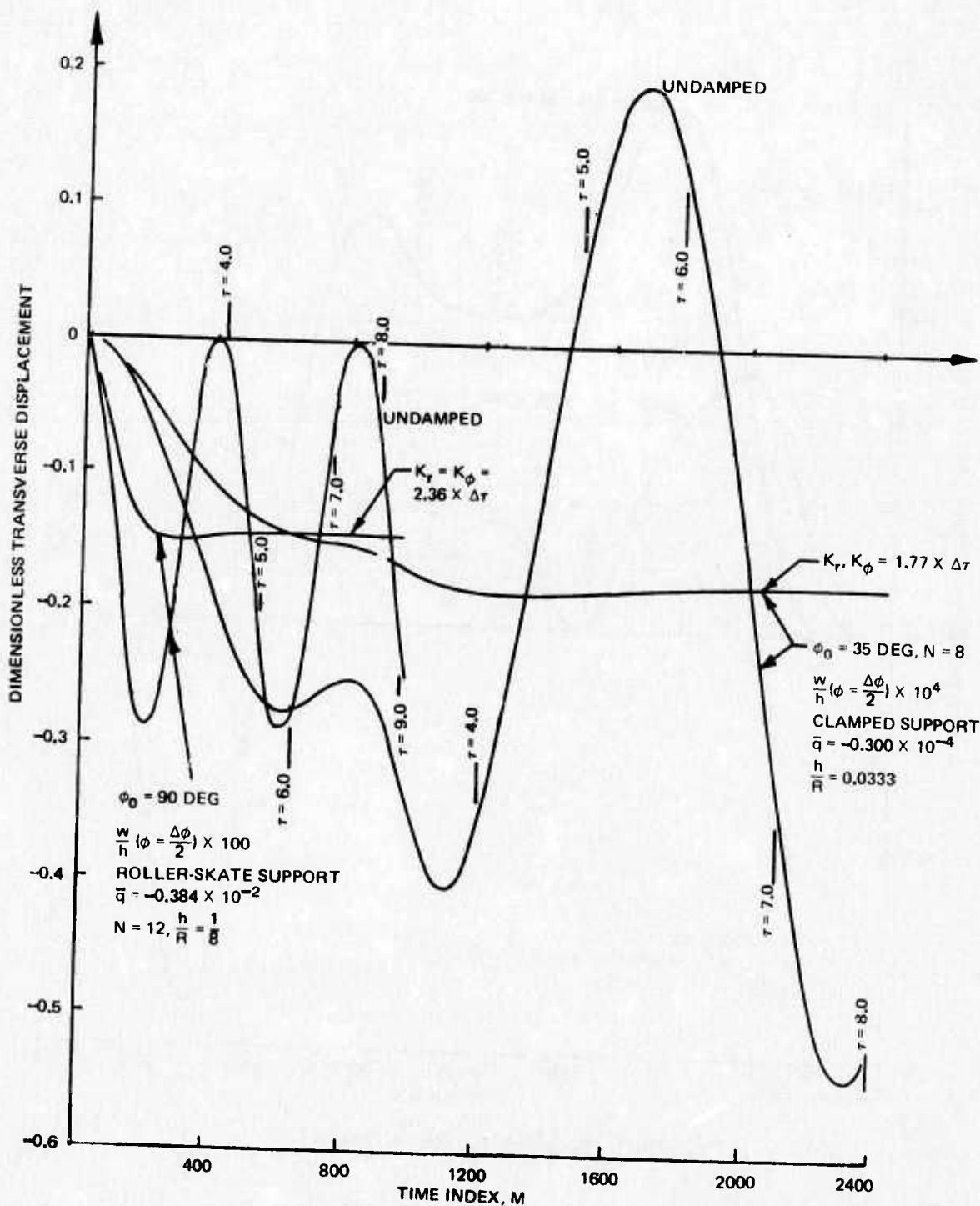


FIGURE 7. Transverse Displacement Versus Time.

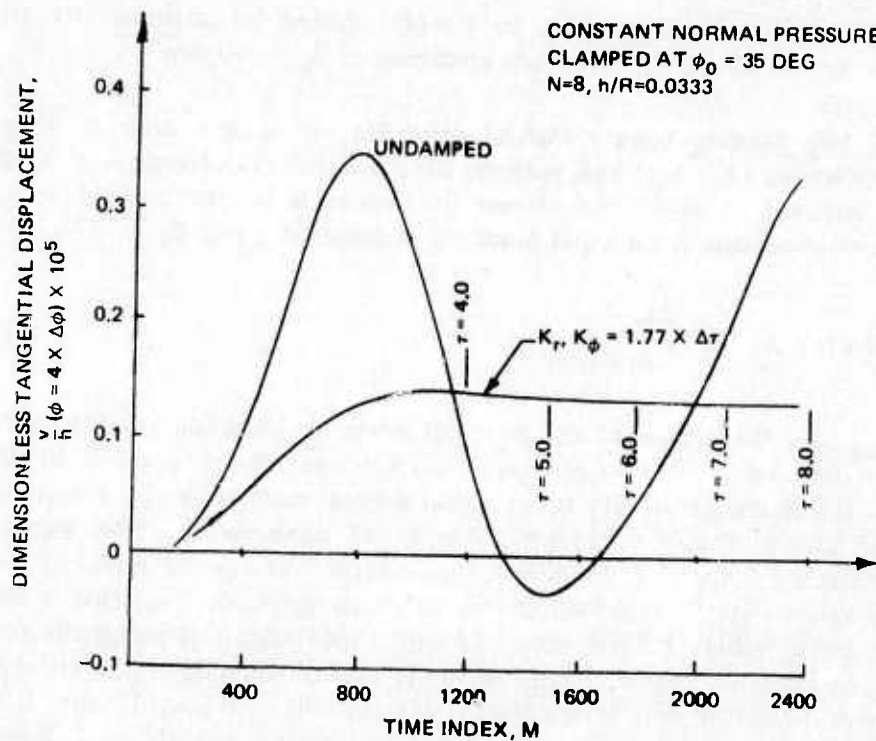


FIGURE 8. Tangential Displacement Versus Time.

The effects of boundary condition and opening angle can be seen by comparing the responses shown on Figures 5 and 7. It is apparent that the stiffening effect of the clamped support at $\phi_0 = 35$ deg substantially lowers the period of the lowest mode of vibration. Further, there are only two local maximas in the 35-deg shell response prior to crossing the axis in comparison to three local maximas for the 90-deg shell. Thus, a running time corresponding to $\tau \approx 8$ should be adequate to span 1 1/2 periods for a shell clamped at $\phi_0 = 35$ deg.

It can be shown that the effect of replacing the clamped support by a simple support at the same value of opening angle and thickness ratio is insignificant and does not warrant any special attention. However, as can be seen from Figure 7, a dramatic effect is achieved in the transverse displacement response if one replaces the clamped support at $\phi_0 = 90$ deg with a roller-skate support. As the tangential displacement is identically zero, the breathing mode only has been excited, and this corresponds to a dimensionless period of approximately $400 (\pm 20) \times \Delta\tau = 3.73 \pm 0.19$. This result compares well with the prediction given by Kraus⁶ that

$$\tau_{\text{PERIOD}} = 2\pi\sqrt{\frac{1-\nu}{2}} = 3.84(\nu=1/4)$$

⁶ Kraus, H. *Thin Elastic Shells*, John Wiley Book Co., 1967.

Thus, a running time corresponding to $\tau \approx 600$ should be adequate to span about 1 1/2 periods for a roller-skate boundary condition at $\phi_0 = 90$ deg.

With the running time (MMAX) identified, it is left only to estimate the damping coefficients (K_r, K_ϕ) and perform an additional calculation with $K_r, K_\phi \neq 0$ to obtain the required solution. As shown in Appendix B, the critical value of the damping factor governing a principal mode of vibration is given by

$$K_{\text{CRITICAL}} = 4\pi \frac{\Delta\tau}{\tau_{\text{PERIOD}}}$$

where τ_{PERIOD} is the period of the principal mode. In choosing a value for K_r, K_ϕ , it has been recommended (footnotes 1 and 2) that one choose a value 70-80% of the critical value. This choice results in an underdamped motion in the lowest mode that exhibits oscillations about the ultimate point of convergence. This behavior is illustrated in Figure 9 for the transverse displacement. As can be seen, the final value ($M = \text{MMAX}$) varies slightly with the choice of damping factor, and that a lower value of damping yields a higher final value. Generally speaking, it is preferable to choose a lower value of damping factor as one can more readily estimate the value about which the solution is oscillating and to which the solution will converge. Finally, it should be noted that no advantage could be gained by choosing K_r, K_ϕ different, based on the

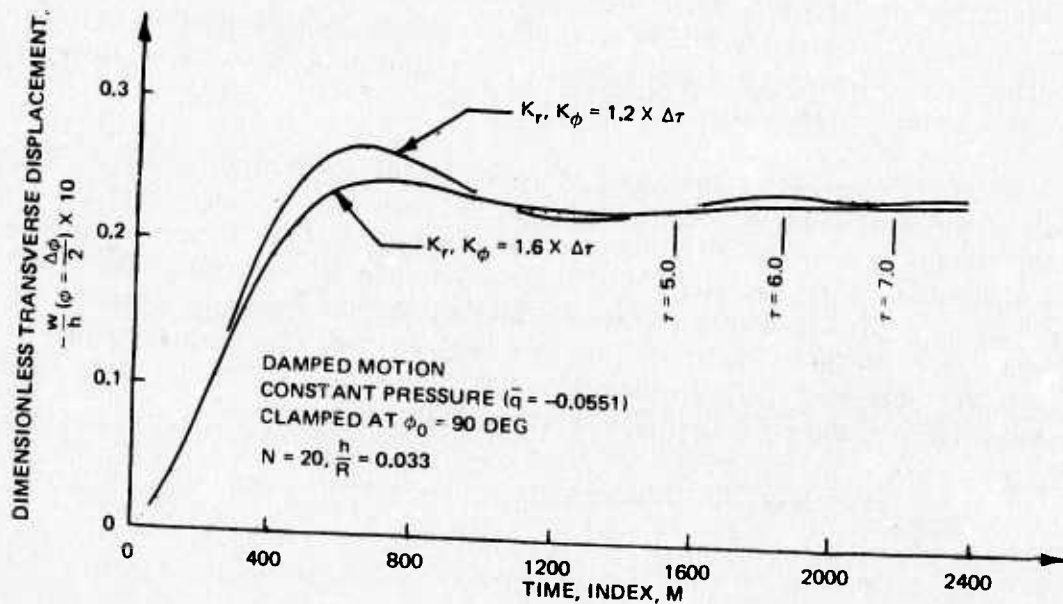


FIGURE 9. Transverse Displacement Versus Time.

observation that the frequency of the coupled mode was lower than that of the breathing mode. Thus, K_r, K_ϕ are chosen equal and inversely proportional to the lowest period of vibration in all calculations.

At this stage, one can choose the output control parameter IPRNT=1 and obtain the complete solution at M=MMAX, and the damped displacement response to use as a check for convergence. However, if one has sufficient confidence in the choice of damping coefficient, IPRNT can be set equal to 2 and only the final solution will be obtained.

Examples of displacement and stress distributions are presented in Figures 10 through 12 for a shell of thickness ratio $\bar{h} = 1/8$, clamped at $\phi_0 = 90$ deg and heated uniformly ($\bar{T}_m = 0.060$). As expected, the results indicate an edge-effect; the significant stress distribution is confined to a region near the restrained edge. Quantitatively, the stresses seem to die out in a distance of about three characteristic lengths (\sqrt{hR}) from the clamped edge. This confirms the recommendation made earlier in choosing a value of N.

Accuracy of THIN

The accuracy of THIN can be assessed by comparing its predictions with exact solutions of the governing equations. However, since there are very few exact solutions available (which are of any real interest), there are a number of solutions whose accuracy can be estimated and therefore can qualify as a standard for comparison.

One exact solution which is meaningful is the membrane state corresponding to uniform normal pressure and supported at the edge so as to restrain the tangential displacement and not induce any bending. This solution can be expressed in the form

$$\bar{w} = \frac{1-\nu}{2} \bar{q} \quad \bar{N}_\phi, \bar{N}_\theta = \frac{1-\nu^2}{2} \bar{q} \quad \bar{v}, \bar{Q}, \bar{M}_\phi, \bar{M}_\theta = 0$$

This state can be achieved with THIN by using the roller-skate support, and leads to

$$\bar{w} = -0.1440 \times 10^{-2} \quad \bar{N}_\phi, \bar{N}_\theta = -0.1800 \times 10^{-2} \quad \bar{M}_\phi, \bar{M}_\theta = 0.000$$

for all stations. The program parameters used in this solution were

$$N = 12 \quad \phi_0 = 90 \text{ deg} \quad \nu = 1/4 \quad \bar{h} = 1/8 \quad \bar{q} = -0.384 \times 10^{-2}$$

$$K_r, K_\phi = 0.0220 \quad \text{MMAX} = 1000$$

As can be seen, the agreement is perfect.

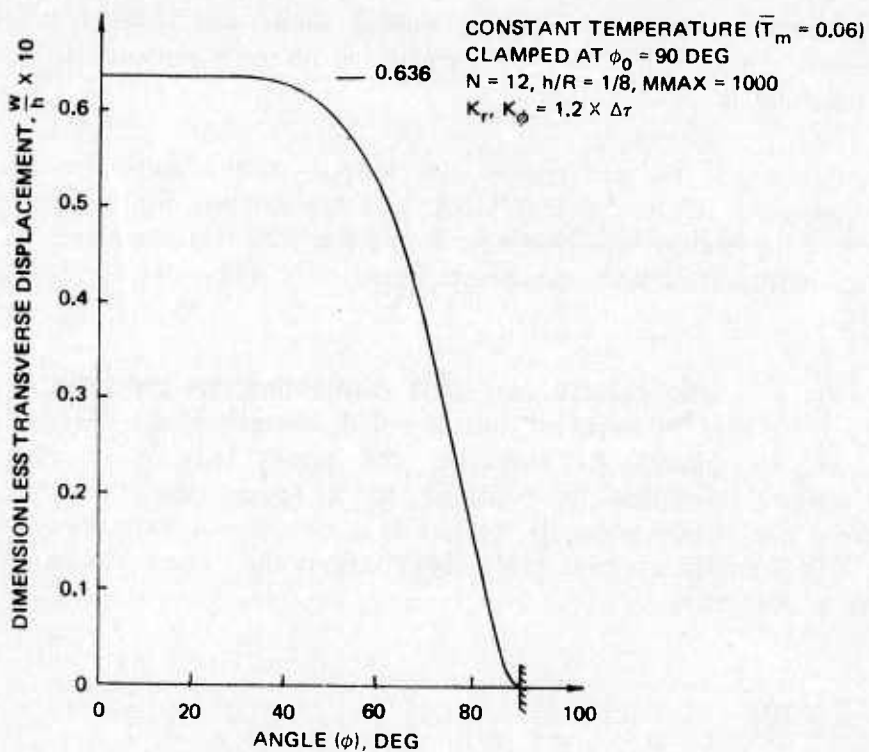


FIGURE 10. Transverse Displacement Distribution.

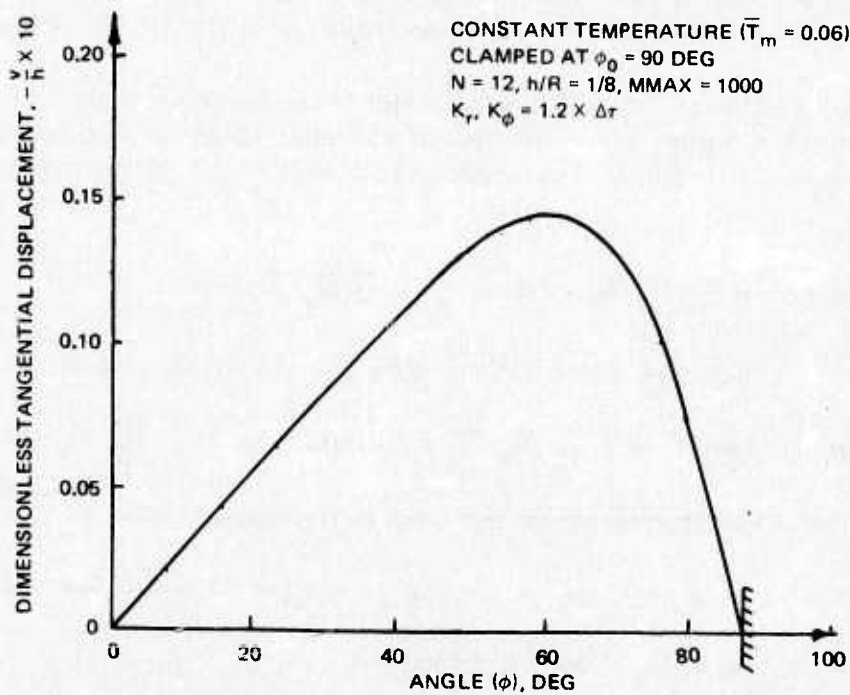


FIGURE 11. Tangential Displacement Distribution.

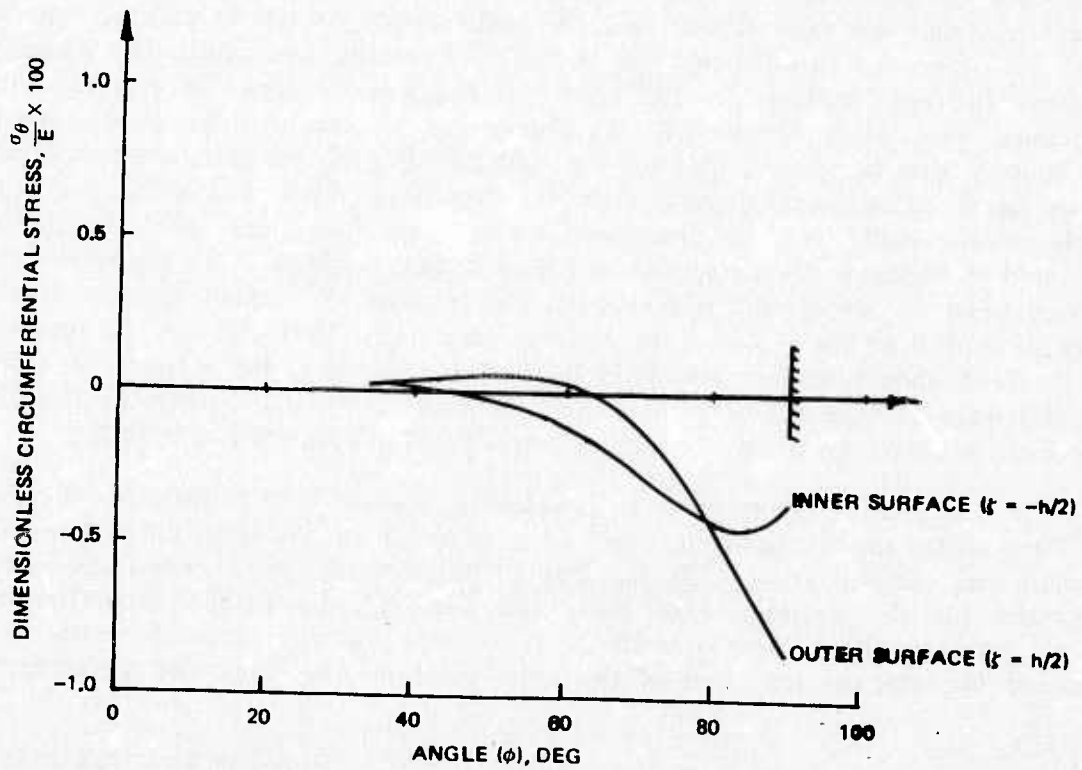
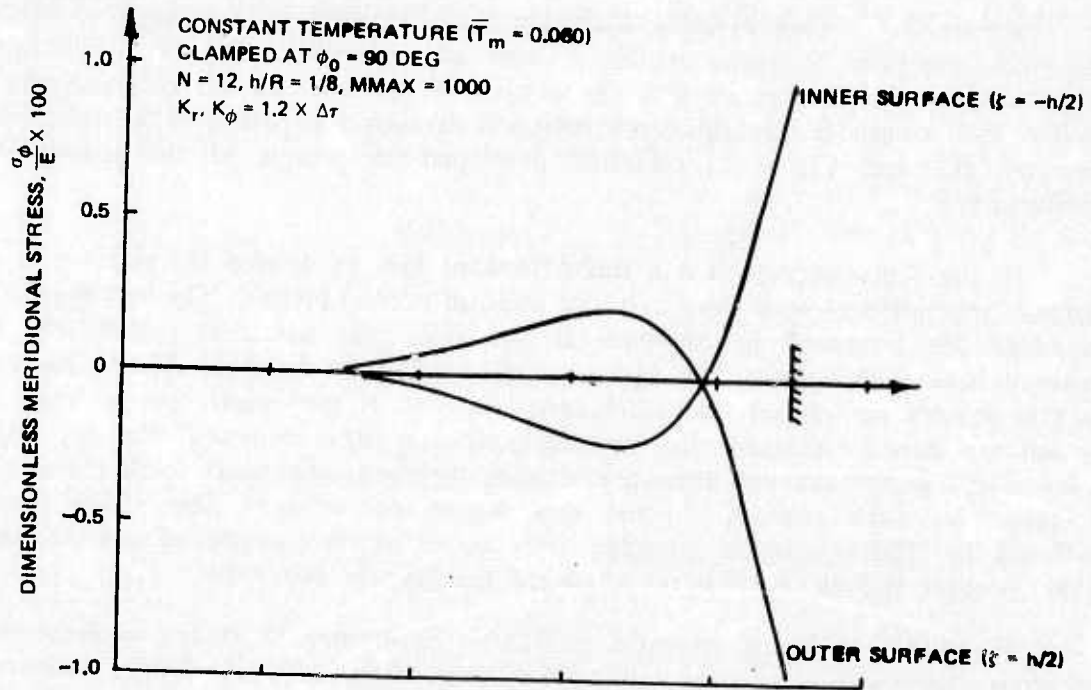


FIGURE 12. Normal Stresses Along Inner, Outer Surfaces.

Besides this simple example, there are (to this writer's knowledge) no other convenient analytical solutions available. There are, however, some series solutions whose accuracy should improve with the number of terms considered. These solutions fall into two categories: (1) asymptotic solutions developed in powers of the thickness parameter (\bar{h}) and (2) series solutions developed in powers of the meridional coordinate (ϕ).

In the first category, it is a straightforward task to develop the solution for a clamped hemispherical shell acted upon by uniform normal pressure. The details of the procedure are presented in Appendix E and only the numerical results will be discussed here. Although the convergence of the solution to the exact solution has not (to this writer's knowledge) been established, one can at least assert that the error in the solution should decrease as the thickness parameter (\bar{h}) is decreased. For very small \bar{h} , we would expect that the difference between the (unknown) exact solution and the two-term asymptotic solution presented here should also be small. Thus, if the results predicted by THIN compare favorably with those of the asymptotic solution, one could conclude that the error in the numerical process was also small.

Numerical results are presented in Figures 13 through 15 for the displacements and circumferential normal stress resultant obtained from THIN and from a two-term, uniformly valid asymptotic solution (UVS) corresponding to thickness parameters (\bar{h}) of 1/8, 1/16, 0.033. The meridional normal stress resultant (N_ϕ/Rp_r) was not plotted since both the predictions of THIN and the UVS varied only insignificantly from each other and from the value 0.5000 over the entire range ($0 \leq \phi \leq 90$ deg). As can be seen, the agreement between the two methods is generally satisfactory. The disparity between the two methods for the transverse displacement seems to increase with decreasing values of \bar{h} . Alternatively, the disparity in the tangential displacement seems not to vary with \bar{h} , and the UVS for the circumferential normal stress resultant is not shown as it differed imperceptibly from the results of THIN. The behavior of the displacement results can be understood when considered along with the results presented in Figure 9. As can be seen in Figure 9, the amplitude of the oscillation still existing when the iterations were terminated was of order 3%. Further, the final results seem to depend on the choice of the damping parameters. Thus, although the accuracy of the UVS should be increasing with decreasing value of \bar{h} , the accuracy of THIN would always be expected to be limited to the range 2-3%. It is noteworthy that the agreement between the results for the stress resultant N_θ does not vary with \bar{h} .

For a solution in the power series category, one can refer to the example given by Timoshenko and Woinowsky-Krieger⁷ for a spherical cap loaded by uniform normal pressure and clamped at $\phi_0 = 35$ deg. The analytical details are described and curves presented for the distribution of meridional bending moment and circumferential normal stress resultant (due to bending). It is noted that the numerical results were obtained by summing ten terms of the series solution. The implication seems to be

⁷ Timoshenko, S. P. and S. Woinowsky-Krieger. *Theory of Plates and Shells*, 2nd Edition, McGraw-Hill, 1959.

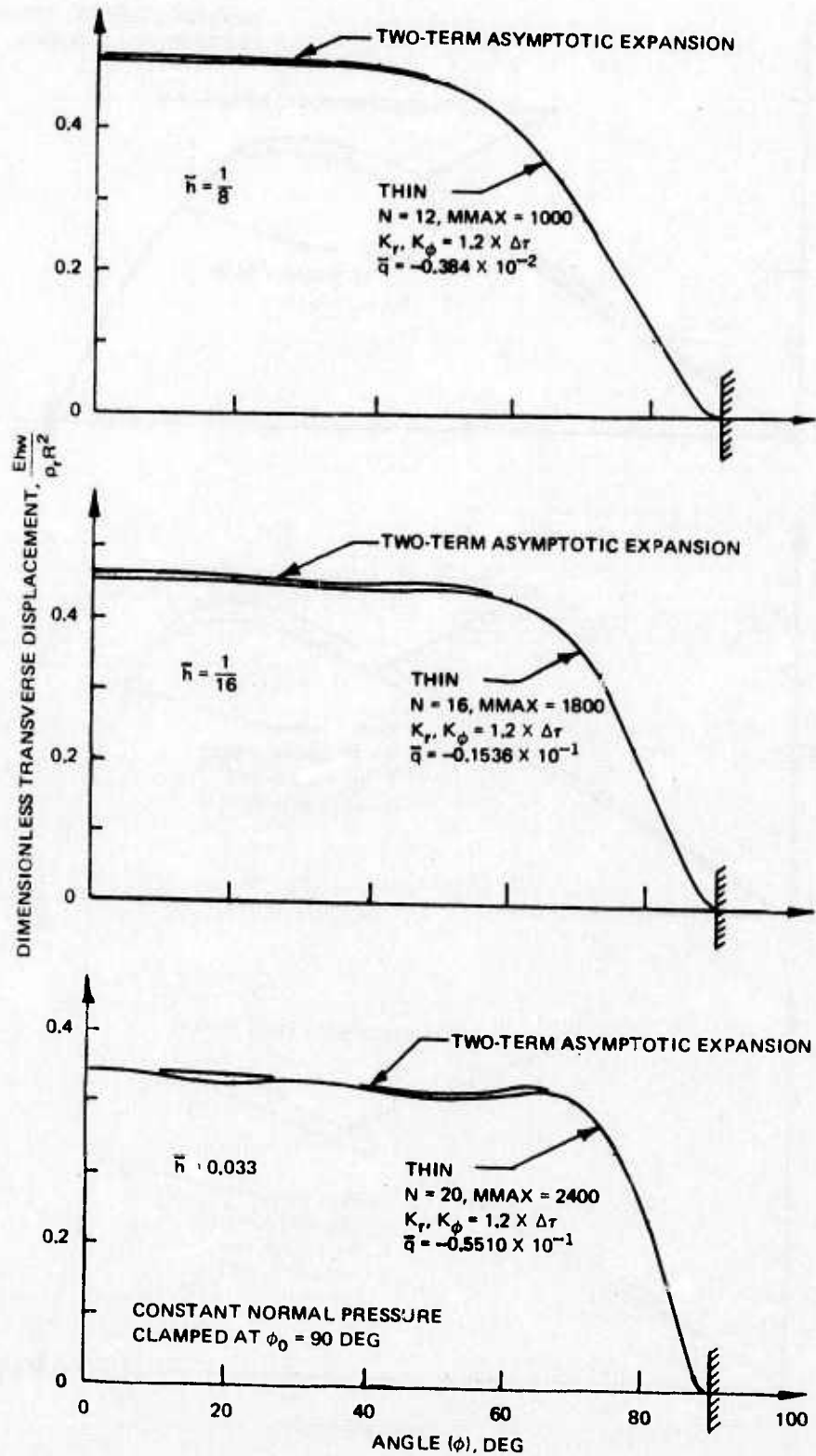


FIGURE 13. Transverse Displacement Distribution.

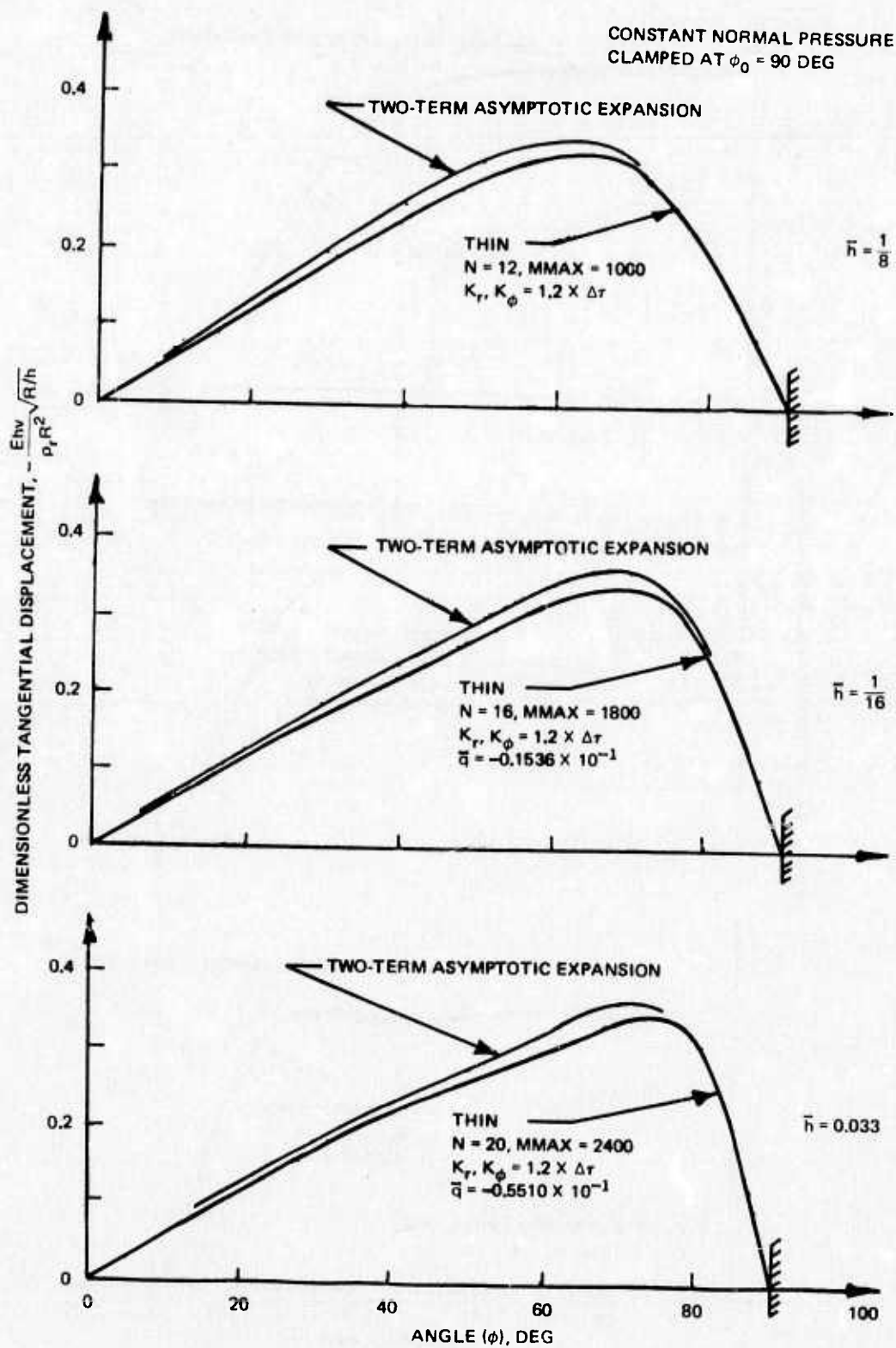


FIGURE 14. Tangential Displacement Distribution.

CONSTANT PRESSURE
CLAMPED AT $\phi_0 = 90$ DEG

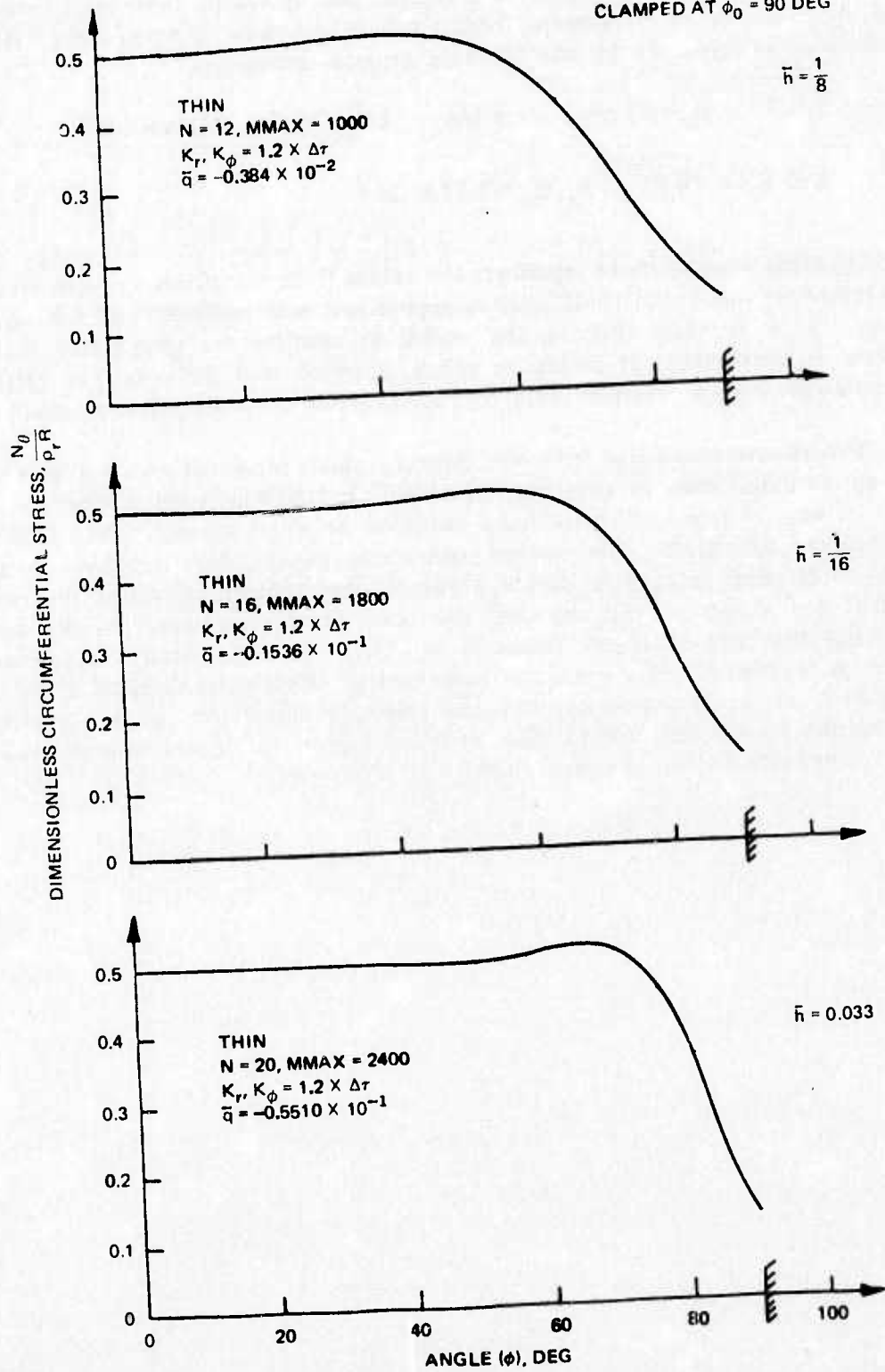


FIGURE 15. Circumferential Stress Resultant.

that the authors considered this to be adequate, and, therefore, these results should be useful as a standard of comparison. Similar results have been obtained using THIN and are presented in Figure 16 for the following program parameters:

$$N = 8 \quad \phi_0 = 35 \text{ deg} \quad \nu = 1/6 \quad \bar{h} = 1/30 \quad \text{MMAX} = 2400$$

$$\bar{q} = -0.3 \times 10^{-4} \quad K_r, K_\phi = 1.77 \times \Delta\tau$$

No attempt has been made to reproduce the curves from Timoshenko's work since the figures there are small and could only be reproduced with difficulty and with dubious accuracy. It is therefore left to the reader to confirm the observation that the agreement is satisfactory. It should be noted, however, that the results of THIN for the meridional bending moment seem to underestimate the edge value by about 10%.

The general conclusion from the three examples presented above is that THIN offers an accurate means of obtaining the stresses and displacements in spherical shells with a variety of boundary conditions enforced on edges ranging from shallow to hemispherical. Admittedly, the loading conditions studied here (uniform pressure, uniform temperature rise) were simple. However, the restraint applied at the edge in each case (see Figure 15, for example) produced a boundary layer (rapidly varying stress state) that was accurately predicted by THIN. As this boundary layer can be regarded as an example of a singular solution out of which more complex stress states can be built up by superposition, one can conclude that THIN has the capacity of predicting the stress states due to more complex loading conditions with an accuracy at least comparable to that obtained above.

NWC TP 5785

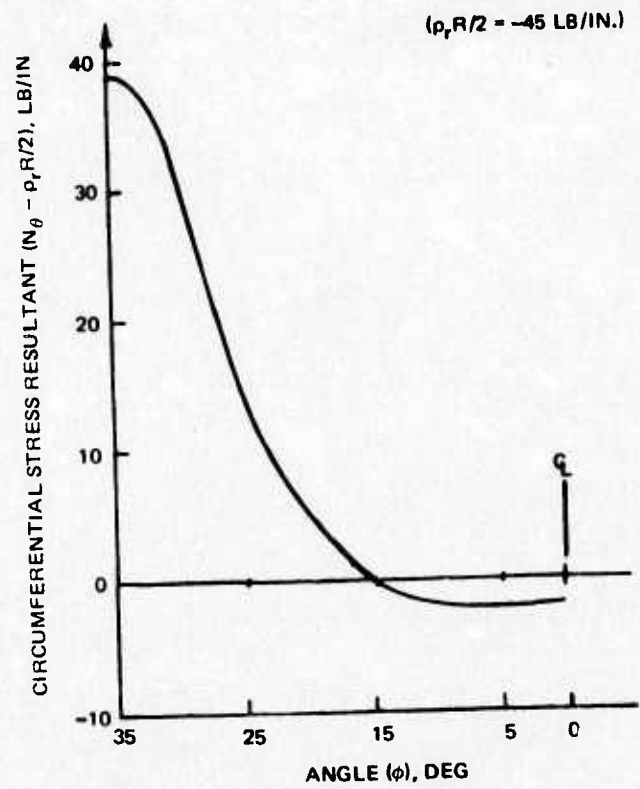
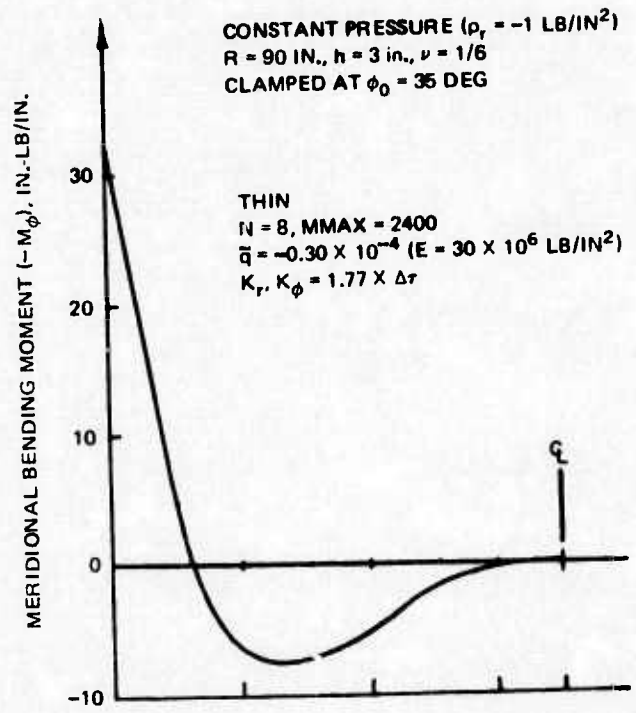


FIGURE 16. Meridional Bending Moment and Circumferential Stress Resultant Due to Bending.

Blank
28

Appendix A
THE GOVERNING EQUATIONS

The governing equations are taken from sections of the *Handbook of Engineering Mechanics* (footnote 4). The notation used here is that of Chapters 40 and 43, although the equations are first made dimensionless before being written into THIN.

If time (t) is scaled such that

$$\tau = \frac{t}{R} \sqrt{\frac{E}{\rho}}$$

and the displacements, strains, rotations and stress resultants are made dimensionless by the introduction of

$$\begin{aligned} (v, w) &= h(\bar{v}, \bar{w}) & (\epsilon_\phi^{(0)}, \epsilon_\theta^{(0)}) &= h(\bar{\epsilon}_\phi, \bar{\epsilon}_\theta)/R \\ X &= h\bar{X}/R & (\kappa_\phi, \kappa_\theta) &= h(\bar{\kappa}_\phi, \bar{\kappa}_\theta)/R^2 \\ (N_\phi, N_\theta) &= hD(\bar{N}_\phi, \bar{N}_\theta)/R & (M_\phi, M_\theta) &= hK(\bar{M}_\phi, \bar{M}_\theta)/R^2 \\ Q_\phi &= hK\bar{Q}/R^3 & (p_r, p_\phi) &= Eh^2(\bar{q}, \bar{p})/R^2 \\ \alpha T_m &= h\bar{T}_m/(R(1+\nu)) & \alpha\Theta &= h\bar{\Theta}/(R^2(1+\nu)) \end{aligned}$$

where

$$\begin{aligned} D &= Eh/(1-\nu^2) & T_m &= \frac{1}{h} \int_{-h/2}^{h/2} (T - T_{REF}) d\xi \\ K &= Eh^3/(12(1-\nu^2)) & \Theta &= \frac{12}{h^3} \int_{-h/2}^{h/2} (T - T_{REF}) \xi d\xi \\ (K_r, K_\phi) &= \omega R^2 \Delta\tau(k_r, k_\phi)/Eh \end{aligned}$$

it follows that the governing equations summarized in footnote 4 become

$$\begin{aligned} \bar{\epsilon}_\phi &= \bar{w} + \frac{\partial \bar{v}}{\partial \phi} & \bar{\epsilon}_\theta &= \bar{w} + \bar{v} \cot \phi \\ \bar{X} &= \frac{\partial \bar{w}}{\partial \phi} - \bar{v} & \bar{\kappa}_\phi &= \frac{\partial \bar{X}}{\partial \phi} & \bar{\kappa}_\theta &= \bar{X} \cot \phi \\ (\bar{N}_\phi, \bar{N}_\theta) &= (\bar{\epsilon}_\phi, \bar{\epsilon}_\theta) + \nu(\bar{\epsilon}_\theta, \bar{\epsilon}_\phi) - T_m \end{aligned}$$

$$(\bar{M}_\phi, \bar{M}_\theta) = (\bar{\kappa}_\phi, \bar{\kappa}_\theta) + \nu(\bar{\kappa}_\theta, \bar{\kappa}_\phi) + \bar{\Theta}$$

$$\bar{Q} = \frac{\partial \bar{M}_\phi}{\partial \phi} + (\bar{M}_\phi - \bar{M}_\theta) \cot \phi$$

$$\frac{\partial^2 \bar{w}}{\partial \tau^2} + \frac{K_r}{\Delta \tau} \frac{\partial \bar{w}}{\partial \tau} = \bar{q} - \frac{1}{1-\nu^2} \left[\bar{N}_\phi + \bar{N}_\theta + \frac{\bar{h}^2}{12} \left(\frac{\partial \bar{Q}}{\partial \phi} + \bar{Q} \cot \phi \right) \right]$$

$$\frac{\partial^2 \bar{v}}{\partial \tau^2} + \frac{K_\phi}{\Delta \tau} \frac{\partial \bar{v}}{\partial \tau} = \bar{p} + \frac{1}{1-\nu^2} \left[\frac{\partial \bar{N}_\phi}{\partial \phi} + (\bar{N}_\phi - \bar{N}_\theta) \cot \phi - \frac{\bar{h}^2}{12} \bar{Q} \right]$$

The dynamic terms are obtained by replacing the radial, tangential components of the distributed surface pressure p_r, p_ϕ (see Figure 1) by

$$p_r - \rho h \frac{\partial^2 w}{\partial t^2} - k_r \frac{\partial w}{\partial t} \qquad p_\phi - \rho h \frac{\partial^2 v}{\partial t^2} - k_\phi \frac{\partial v}{\partial t}$$

respectively, where ρ is the mass density, and k_r, k_ϕ are the (fictitious) damping factors (load/area/velocity) in the radial, tangential directions, respectively.

Appendix B
CRITICAL DAMPING FACTOR

Following Appendix A, it can be seen that the governing equation for $\bar{w}(\phi, \tau)$ has the form

$$\frac{\partial^2 \bar{w}}{\partial \tau^2} + \frac{K_r}{\Delta \tau} \frac{\partial \bar{w}}{\partial \tau} = A(\phi, \tau)$$

If we look for solutions by the separation of variables technique, i.e., assume

$$(\bar{w}, A) = (W, A) \exp(i\Omega\tau)$$

where W, A are functions of ϕ only, we find on substitution that the frequency factor Ω is governed by

$$\Omega = \frac{1}{2} \left\{ \frac{iK_r}{\Delta \tau} \pm \sqrt{4\Omega_0^2 - (K_r/\Delta \tau)^2} \right\}$$

where $\Omega_0^2 = -A/W$. The critical value of K_r is such that the term in the square root bracket vanishes, i.e.,

$$(K_r)_{\text{CRITICAL}} = 2\Omega_0 \Delta \tau$$

If we now identify Ω_0 as the frequency of the lowest mode of free ($K_r = 0$) vibration, then

$$\Omega_0 \tau_{\text{PERIOD}} = 2\pi$$

and

$$(K_r)_{\text{CRITICAL}} = 4\pi \frac{\Delta \tau}{\tau_{\text{PERIOD}}}$$

b/2nK
32

Appendix C
THE TEMPERATURE INTEGRALS

In this section, formulae will be derived for the numerical evaluation of the temperature integrals T_m , Θ which appear in the constitutive equations. It is assumed that temperature data are available at each meridional station at five equally spaced points through the thickness (see Figure 4) not including the end points of the interval. This latter restriction arises from the fact that temperatures are generally computed using an algorithm based on energy balances applied to regions of space. If these regions are chosen of equal thickness, the temperatures are naturally obtained at the points noted in Figure 4. Alternatively, should the temperatures be defined at equally spaced points through the thickness including the end points of the interval, the equations given below can be replaced by the well-known Newton-Cotes formulae.

Assuming now that the temperatures are defined as shown in Figure 4, we begin by attempting to represent the temperature distribution by the polynomial

$$T(\bar{\zeta}) = a_0 + a_1 \bar{\zeta} + a_2 \bar{\zeta}^2 + a_3 \bar{\zeta}^3 + a_4 \bar{\zeta}^4 \quad \left(\bar{\zeta} = \zeta/h, -\frac{1}{2} \leq \bar{\zeta} \leq \frac{1}{2} \right)$$

and evaluate the coefficients a_0, \dots, a_4 so that

$$T_1 = T(-0.4) = a_0 - 0.4a_1 + 0.4^2 a_2 - 0.4^3 a_3 + 0.4^4 a_4$$

$$T_2 = T(-0.2) = a_0 - 0.2a_1 + 0.2^2 a_2 - 0.2^3 a_3 + 0.2^4 a_4$$

$$T_3 = T(0) = a_0$$

$$T_4 = T(0.2) = a_0 + 0.2a_1 + 0.2^2 a_2 + 0.2^3 a_3 + 0.2^4 a_4$$

$$T_5 = T(0.4) = a_0 + 0.4a_1 + 0.4^2 a_2 + 0.4^3 a_3 + 0.4^4 a_4$$

The coefficients are readily obtained from equations obtained by adding and subtracting the first and last pairs of the equations given above so as to separate the unknowns a_2, a_4 and a_1, a_3 .

It then follows that

$$a_1 = (T_1 - 8T_2 + 8T_4 - T_5)/2.4$$

$$a_2 = (-T_1 + 16T_2 - 30T_3 + 16T_4 - T_5)/0.96$$

$$a_3 = (-T_1 + 2T_2 - 2T_4 + T_5)/0.096$$

$$a_4 = (T_1 - 4T_2 + 6T_3 - 4T_4 + T_5)/0.0384$$

Further, with the result that

$$T_m + T_{REF} = a_0 + a_2/12 + a_4/80$$

$$h\Theta = a_1 + 3a_3/20$$

we obtain

$$\bar{T}_m = (1+\nu)\frac{\alpha}{h} \left[(275T_1 + 100T_2 + 402T_3 + 100T_4 + 275T_5)/1152 - T_{REF} \right]$$

$$\bar{\Theta} = 5(1+\nu)\frac{\alpha}{h^2} (-11T_1 - 2T_2 + 2T_4 + 11T_5)/48$$

Appendix D
THE STRESS DISTRIBUTION

In this section, formulae will be derived for the meridional, circumferential components of the in-plane, normal stress that are consistent with the definitions of the stress resultants and the sign convention shown in Figure 1.

Let us begin by defining the meridional, circumferential components of strain at an arbitrary point (ϕ, ζ) in the shell as follows

$$\epsilon_{\phi} = \epsilon_{\phi}^{(0)}(\phi) - \zeta \kappa_{\phi}(\phi)$$

$$\epsilon_{\theta} = \epsilon_{\theta}^{(0)}(\phi) - \zeta \kappa_{\theta}(\phi)$$

Further, let the stress resultants N_i, M_i be defined as integrals of the appropriate components of normal stress through the thickness of the shell with the convention that

$$(N_{\phi}, N_{\theta}) = \int_{-h/2}^{h/2} (\sigma_{\phi\phi}, \sigma_{\theta\theta}) d\zeta$$

$$(M_{\phi}, M_{\theta}) = - \int_{-h/2}^{h/2} (\sigma_{\phi\phi}, \sigma_{\theta\theta}) \zeta d\zeta$$

Finally, if the state of stress in the shell is nearly that corresponding to plane stress ($\sigma_{\zeta\zeta} = 0$), then Hooke's Law takes the form

$$\epsilon_{\phi} = (\sigma_{\phi\phi} - \nu\sigma_{\theta\theta})/E + \alpha(T - T_{REF})$$

$$\epsilon_{\theta} = (\sigma_{\theta\theta} - \nu\sigma_{\phi\phi})/E + \alpha(T - T_{REF})$$

Alternatively,

$$\sigma_{\phi\phi} = E(\epsilon_{\phi} + \nu\epsilon_{\theta})/(1-\nu^2) - \alpha E(T - T_{REF})/(1-\nu)$$

$$\sigma_{\theta\theta} = E(\epsilon_{\theta} + \nu\epsilon_{\phi})/(1-\nu^2) - \alpha E(T - T_{REF})/(1-\nu)$$

These equations can be rearranged in a number of ways to suit one's convenience.

If the equations for $\sigma_{\phi\phi}, \sigma_{\theta\theta}$ are substituted into the definitions of the stress resultants, and we further substitute the expressions for the strain components at a general point in terms of the middle-surface strains ($\epsilon_{\phi}^{(0)}, \epsilon_{\theta}^{(0)}$) and curvatures ($\kappa_{\phi}, \kappa_{\theta}$) we obtain the following constitutive equations

$$N_{\phi} = D[\epsilon_{\phi}^{(0)} + \nu\epsilon_{\theta}^{(0)} - (1+\nu)\alpha T_m]$$

$$N_{\theta} = D[\epsilon_{\theta}^{(0)} + \nu\epsilon_{\phi}^{(0)} - (1+\nu)\alpha T_m]$$

$$M_{\phi} = K[\kappa_{\phi} + \nu\kappa_{\theta} + (1+\nu)\alpha\Theta]$$

$$M_{\theta} = K[\kappa_{\theta} + \nu\kappa_{\phi} + (1+\nu)\alpha\Theta]$$

which are consistent with those equations noted in Appendix A. These equations can be rearranged to yield the following strain-force stress resultant, curvature-moment stress resultant equations:

$$\epsilon_{\phi}^{(0)} = (N_{\phi} - \nu N_{\theta})/Eh + \alpha T_m$$

$$\epsilon_{\theta}^{(0)} = (N_{\theta} - \nu N_{\phi})/Eh + \alpha T_m$$

$$\kappa_{\phi} = 12(M_{\phi} - \nu M_{\theta})/Eh^3 - \alpha\Theta$$

$$\kappa_{\theta} = 12(M_{\theta} - \nu M_{\phi})/Eh^3 - \alpha\Theta$$

Finally, if these expressions for the strain, curvature components are substituted into Hooke's Law, we obtain the following expressions for the in-plane stresses

$$\sigma_{\phi\phi}/E = N_{\phi}/Eh - 12\xi M_{\phi}/Eh^3 - \alpha(T - T_m - T_{REF} - \xi\Theta)/(1-\nu)$$

$$\sigma_{\theta\theta}/E = N_{\theta}/Eh - 12\xi M_{\theta}/Eh^3 - \alpha(T - T_m - T_{REF} - \xi\Theta)/(1-\nu)$$

When expressed in dimensionless variables, these equations become

$$\sigma_{\phi\phi}/E = \bar{h}[\bar{N}_{\phi} + \bar{T}_m - \xi\bar{h}(\bar{M}_{\phi} - \bar{\Theta})]/(1-\nu^2) - \alpha(T - T_{REF})/(1-\nu)$$

$$\sigma_{\theta\theta}/E = \bar{h}[\bar{N}_{\theta} + \bar{T}_m - \xi\bar{h}(\bar{M}_{\theta} - \bar{\Theta})]/(1-\nu^2) - \alpha(T - T_{REF})/(1-\nu)$$

Appendix E
ASYMPTOTIC SOLUTION FOR A THIN SHELL

In this section, we consider the problem of determining the deflections, stresses in a clamped hemispherical shell that is loaded by a uniform distribution of normal pressure. In particular, we will seek a solution as a sequence of solutions, each term in the sequence multiplied by an ever increasing power of the thickness parameter (\bar{h}), so that (one expects) the accuracy of the solution at any stage should increase as the number of terms in the sequence is increased. Although this method of constructing solutions is described in a number of texts, we will refer here to the formalism described by Cole.⁸

The problem we wish to consider is described by the equations presented in Appendix A where we take $p_r = \text{constant}$ and delete all temperature terms. We wish to obtain a solution subject to the boundary conditions that

$$v, w, X = 0 \qquad \phi = \phi_0$$

As a starting point, we observe that the following membrane state

$$\begin{aligned} N_\phi, N_\theta &= p_r R/2 & X, M_\phi, M_\theta, Q_\phi &= 0 \\ v &= C^{(0)} \sin \phi & w &= \frac{1-\nu}{Eh} \frac{p_r R^2}{2} - C^{(0)} \cos \phi \end{aligned}$$

is an exact solution of the governing equations, although it does not satisfy the boundary conditions. Physically, we expect that the solution we seek should behave like this membrane state in regions of the shell that are not near the edge. What is required, therefore, is a solution that is valid near the edge, satisfies the boundary conditions and converges to the membrane state in some sense for ϕ such that $\phi < \phi_0$.

In this edge region, we expect a rapid variation with distance for the dependent variables. In particular, we assume that the dependent variables may vary significantly over a distance comparable with the characteristic length (\sqrt{Rh}), and define a dimensionless length scale (ξ), measured from the edge, given by

$$\phi = \phi_0 - \epsilon \xi \qquad \epsilon^2 = \bar{h}$$

Let us further adopt the following set of dimensionless variables

$$\begin{aligned} v &= \epsilon p_r R^2 \hat{v}/Eh & w &= p_r R^2 \hat{w}/Eh \\ (N_\phi, N_\theta, Q_\phi) &= p_r R (\hat{N}_\phi, \hat{N}_\theta, \epsilon \hat{Q}) \end{aligned}$$

⁸ Cole, J. D. *Perturbation Methods in Applied Mathematics*, Blaisdell Publishing Co., 1968.

$$(M_\phi, M_\theta) = p_1 h^2 (\widehat{M}_\phi, \widehat{M}_\theta) / (12\epsilon^2(1-\nu^2))$$

In these variables, we can develop the governing equations in the following form

$$(1-\nu^2)(\widehat{N}_\phi, \widehat{N}_\theta) = (1+\nu)\widehat{w} - (1, \nu)\frac{d\widehat{v}}{d\xi} + (\nu, 1)\epsilon\widehat{v} \cot \phi + O(\epsilon^3)$$

$$(\widehat{M}_\phi, \widehat{M}_\theta) = (1, \nu)\frac{d^2\widehat{w}}{d\xi^2} - (\nu, 1)\epsilon\frac{d\widehat{w}}{d\xi} \cot \phi + (1, \nu)\epsilon^2\frac{d\widehat{v}}{d\xi} + O(\epsilon^3)$$

$$m^4\widehat{Q}_\phi = -\frac{d\widehat{M}_\phi}{d\xi} + \epsilon(\widehat{M}_\phi - \widehat{M}_\theta) \cot \phi + O(\epsilon^3)$$

$$\frac{d\widehat{N}_\phi}{d\xi} - \epsilon(\widehat{N}_\phi - \widehat{N}_\theta) \cot \phi + \epsilon^2\widehat{Q} + O(\epsilon^3) = 0$$

$$\frac{d\widehat{Q}}{d\xi} - \epsilon\widehat{Q} \cot \phi - (\widehat{N}_\phi + \widehat{N}_\theta) + O(\epsilon^3) = -1$$

where $m^4 = 12(1-\nu^2)$, and

$$\cot \phi = \cot \phi_0 + \epsilon\xi \csc^2 \phi_0 + \epsilon^2 \xi^2 \cot \phi_0 \csc^2 \phi_0 + O(\epsilon^3)$$

as appropriate.

From the form of these equations, it is apparent that expansions of the type

$$\widehat{v}(\epsilon, \xi) = \widehat{v}^{(0)}(\xi) + \epsilon\widehat{v}^{(1)}(\xi) + \epsilon^2\widehat{v}^{(2)}(\xi) + O(\epsilon^3)$$

$$\widehat{w}(\epsilon, \xi) = \widehat{w}^{(0)}(\xi) + \epsilon\widehat{w}^{(1)}(\xi) + \epsilon^2\widehat{w}^{(2)}(\xi) + O(\epsilon^3)$$

$$\widehat{N}_\phi(\epsilon, \xi) = 1/2 + \epsilon n_\phi^{(1)}(\xi) + \epsilon^2 n_\phi^{(2)}(\xi) + O(\epsilon^3)$$

$$\widehat{N}_\theta(\epsilon, \xi) = n_\theta^{(0)}(\xi) + \epsilon n_\theta^{(1)}(\xi) + \epsilon^2 n_\theta^{(2)}(\xi) + O(\epsilon^3)$$

$$\widehat{Q}(\epsilon, \xi) = q^{(0)}(\xi) + \epsilon q^{(1)}(\xi) + \epsilon^2 q^{(2)}(\xi) + O(\epsilon^3)$$

$$\widehat{M}_\phi(\epsilon, \xi) = m_\phi^{(0)}(\xi) + \epsilon m_\phi^{(1)}(\xi) + \epsilon^2 m_\phi^{(2)}(\xi) + O(\epsilon^3)$$

$$\widehat{M}_\theta(\epsilon, \xi) = m_\theta^{(0)}(\xi) + \epsilon m_\theta^{(1)}(\xi) + \epsilon^2 m_\theta^{(2)}(\xi) + O(\epsilon^3)$$

should exist. The constant (1/2) as the leading term in the expansion for \widehat{N}_ϕ anticipates the requirement for zero order matching.

The equations governing the zeroth, first and higher order terms in the above expansions are obtained by substituting these expansions into the governing equations and taking successive limits of the governing equations as $\epsilon \rightarrow 0$ holding ξ -fixed. In particular, we find that

$$\begin{aligned} \frac{d\widehat{v}^{(0)}}{d\xi} &= (1+\nu)\widehat{w}^{(0)} - (1-\nu^2)/2 & m^4 q^{(0)} &= -\frac{dm_\phi^{(0)}}{d\xi} \\ (1-\nu^2)n_\theta^{(0)} &= (1+\nu)\widehat{w}^{(0)} - \nu\frac{d\widehat{v}^{(0)}}{d\xi} & \frac{dq^{(0)}}{d\xi} - n_\theta^{(0)} &= -1/2 \\ m_\phi^{(0)} &= \frac{d^2\widehat{w}^{(0)}}{d\xi^2} & m_\theta^{(0)} &= \nu m_\phi^{(0)} \end{aligned}$$

govern the zeroth order solution, and

$$\begin{aligned} (1-\nu^2)(n_\phi^{(1)}, n_\theta^{(1)}) &= (1+\nu)\widehat{w}^{(1)} - (1, \nu)\frac{d\widehat{v}^{(1)}}{d\xi} + (\nu, 1)\widehat{v}^{(0)} \cot \phi_0 \\ (m_\phi^{(1)}, m_\theta^{(1)}) &= (1, \nu)\frac{d^2\widehat{w}^{(1)}}{d\xi^2} - (\nu, 1)\frac{d\widehat{w}^{(0)}}{d\xi} \cot \phi_0 \\ m^4 q^{(1)} &= -\frac{dm_\phi^{(1)}}{d\xi} + (m_\phi^{(0)} - m_\theta^{(0)}) \cot \phi_0 \\ \frac{dn_\phi^{(1)}}{d\xi} &= (1/2 - n_\theta^{(0)}) \cot \phi_0 \\ \frac{dq^{(1)}}{d\xi} - q^{(0)} \cot \phi_0 - (n_\phi^{(1)} + n_\theta^{(1)}) &= 0 \end{aligned}$$

govern the first order correction, and

$$\begin{aligned} (1-\nu^2)(n_\phi^{(2)}, n_\theta^{(2)}) &= (1+\nu)\widehat{w}^{(2)} - (1, \nu)\frac{d\widehat{v}^{(2)}}{d\xi} + (\nu, 1)\xi\widehat{v}^{(0)} \csc^2 \phi_0 + (\nu, 1)\widehat{v}^{(1)} \cot \phi_0 \\ (m_\phi^{(2)}, m_\theta^{(2)}) &= (1, \nu)\left(\frac{d^2\widehat{w}^{(2)}}{d\xi^2} + \frac{d\widehat{v}^{(0)}}{d\xi}\right) - (\nu, 1)\left(\xi\frac{d\widehat{w}^{(0)}}{d\xi} \csc^2 \phi_0 + \frac{d\widehat{w}^{(1)}}{d\xi} \cot \phi_0\right) \end{aligned}$$

$$m^4 q^{(2)} = -\frac{dm_\phi^{(2)}}{d\xi} + \xi (m_\phi^{(0)} - m_\theta^{(0)}) \csc^2 \phi_0 + (m_\phi^{(1)} - m_\theta^{(1)}) \cot \phi_0$$

$$\frac{dn_\phi^{(2)}}{d\xi} = -q^{(0)} + (1/2 - n_\theta^{(0)}) \xi \csc^2 \phi_0 + (n_\phi^{(1)} - n_\theta^{(1)}) \cot \phi_0$$

$$\frac{dq^{(2)}}{d\xi} - (\xi q^{(0)} \csc^2 \phi_0 + q^{(1)} \cot \phi_0) - (n_\phi^{(2)} + n_\theta^{(2)}) = 0$$

govern the second order correction. In the paragraphs to follow, the solution to the above system of equations will be described which matches the membrane state in the region of the shell that is not near the edge. It will be assumed that the reader is familiar with the matching process so that little of the motivation needs to be described and only the results of the process will be presented. Furthermore, only the case $\phi_0 = 90$ deg will be described.

Thus, in anticipation of the requirement that all solutions be bounded exponentially as $\xi \rightarrow \infty$, we take the zeroth order solution in the form

$$\widehat{w}^{(0)} = (1-\nu)/2 + e^{-x}(A_0 \sin x + B_0 \cos x) \quad x = m\xi/\sqrt{2}$$

$$q^{(0)} = -e^{-x}[(A_0 + B_0) \cos x + (A_0 - B_0) \sin x]/m\sqrt{2}$$

$$\widehat{v}^{(0)} = C_0^{(i)} + (1+\nu)q^{(0)} \quad n_\theta^{(0)} = \nu/2 + \widehat{w}^{(0)}$$

The solution of the equations governing the first order correction can be shown to vanish identically for the case $\phi_0 = 90$ deg. This follows from the anticipated observation that as the governing equations become homogeneous for $\phi_0 = 90$ deg, the only solution which satisfies homogeneous boundary conditions is the trivial solution.

Thus, as we seek more than the first term in the expansion, we must turn our attention to the second order equations. In doing so, we find that

$$\begin{aligned} \widehat{w}^{(2)} = & -(1+\nu)C_2^{(i)} - C_0^{(i)}\xi - 3\xi q^{(0)}/4 + e^{-x}[\xi^2(A_0 \sin x + B_0 \cos x)/4 + \\ & + A_2 \sin x + B_2 \cos x] \end{aligned}$$

$$\widehat{v}^{(2)} = D_2^{(i)} - 2(1+\nu)C_2^{(i)}\xi - C_0^{(i)}\xi^2/2 + \frac{1+\nu}{\sqrt{2}} e^{-x} \left[\sin x \left(\frac{B_2 - A_2}{m} + \frac{A_0 + B_0}{4m^3} + \frac{B_0 x}{2m^3} + \frac{B_0 - A_0}{2m^3} x^2 \right) + \cos x \left(-\frac{A_2 + B_2}{m} + \frac{B_0 - A_0}{4m^3} - \frac{A_0 x}{2m^3} - \frac{A_0 + B_0}{2m^3} x^2 \right) \right]$$

$$n_\phi^{(2)} = \nu n_\phi^{(2)} + \widehat{w}^{(2)} + \xi \widehat{v}^{(0)} \qquad n_\phi^{(2)} = C_2^{(i)} - \xi q^{(0)}$$

The constants $A_0, B_0, C_0^{(i)}, A_2, B_2, C_2^{(i)}, D_2^{(i)}$ of the edge (or inner) solution, and $q^{(0)}$ of the membrane (or outer) solution will now be chosen so as to satisfy either the boundary conditions or the matching requirements.

The boundary conditions at $\phi = 90 \text{ deg } (\xi = 0)$ require that

$$\widehat{w}^{(0)}(0) = \widehat{w}^{(1)}(0) = \widehat{w}^{(2)}(0) = \dots = 0$$

$$\widehat{v}^{(0)}(0) = \widehat{v}^{(1)}(0) = \widehat{v}^{(2)}(0) = \dots = 0$$

$$\frac{d\widehat{w}^{(0)}}{d\xi}(0) = \frac{d\widehat{w}^{(1)}}{d\xi}(0) = \frac{d\widehat{w}^{(2)}}{d\xi}(0) + \widehat{v}^{(0)}(0) = \dots = 0$$

On applying these boundary conditions to the zeroth order solution, we find

$$A_0 = B_0 = -(1-\nu)/2 \qquad C_0^{(i)} = -(1-\nu^2)/\sqrt{2m}$$

Now, before applying the boundary conditions to the second order corrections, it is convenient to obtain the requirements of the matching process.

Following Cole (see footnote 8), we first define an intermediate length scale ξ_η where

$$\xi_\eta = \frac{\phi_0 - \phi}{\eta(\epsilon)} = \xi \epsilon / \eta(\epsilon)$$

and $\eta(\epsilon)$ is such that

$$\lim_{\epsilon \rightarrow 0} \frac{\epsilon}{\eta(\epsilon)} = 0$$

For example, we could choose $\eta = \epsilon^{1/2}$. In what follows, we will require that the edge (or inner) solution, expressed in the intermediate variable, converge to the membrane solution, also expressed in the intermediate variable, for all values of ξ_η (fixed) as $\epsilon \rightarrow 0$.

On applying this matching condition to N_ϕ , we find that $n_\phi^{(1)} = 0$ thus verifying the fact that the first order equations are homogeneous, and

$$\lim_{\epsilon \rightarrow 0, \xi_\eta \text{ - FIXED}} n_\phi^{(2)} = 0$$

so that

$$C_2^{(i)} = 0$$

On applying the matching condition to \hat{v} , we find

$$C^{(o)} = \epsilon p_r R^2 C_0^{(i)} / Eh$$

for zeroth order matching. The remaining constants are found on applying the boundary conditions to the second order correction.

The boundary conditions on $\hat{w}^{(2)}$, $\frac{d\hat{w}^{(2)}}{d\xi}$ are satisfied by taking

$$A_2 = -(1-\nu)(1+4\nu)/4m^2 \quad B_2 = 0$$

The boundary condition on $\hat{v}^{(2)}$ is satisfied by taking

$$D_2^{(i)} = -m(1+4\nu)/48\sqrt{2}$$

This completes the solution as it can be shown that the remaining matching conditions are also satisfied.

As a final remark, it is convenient to obtain the above solution in a form which is uniformly valid over the entire range of opening angle rather than have solutions whose range of validity was restricted. Again Following Cole (footnote 8), such uniformly valid solutions can be constructed by subtracting the *common part* from the sum of the inner and outer solutions. The *common part* of the solution are those terms in both the inner and outer solutions which match identically in the matching process. For the example studied here ($\phi_0 = 90$ deg), it can be shown that uniformly valid, two-term expansions can be constructed in the following form

$$\widehat{w} = \widehat{w}^{(0)} + \epsilon^2 \widehat{w}^{(2)} + \epsilon(1-\nu^2)(\cos \phi - \epsilon \xi) / m\sqrt{2}$$

$$\widehat{v} = \widehat{v}^{(0)} + \epsilon^2 \widehat{v}^{(2)} - (1-\nu^2)(\sin \phi - 1 + \epsilon^2 \xi^2 / 2) / m\sqrt{2}$$

$$\widehat{N}_\phi = 1/2 + \epsilon^2 n_\phi^{(2)}$$

$$\widehat{N}_\theta = n_\theta^{(0)} + \epsilon^2 n_\theta^{(2)}$$

Numerical results obtained from these expressions are presented in Figures 13 through 15 for several values of the thickness parameter.

Blank
44

NWC TP 5785

Appendix F
PROGRAM LISTING

```

C THIN, SPHERICAL SHELL WITH SURFACE LOAD, TEMPERATURE EFFECTS
C SET NBC TO 0 FOR CLAMPED BOUNDARY AT PHI=PO, TO 1 FOR SIMPLY SUPPORTED
C BOUNDARY, TO 2 FOR ROLLER-SKATE BOUNDARY.
C SET IPRNT TO 0 FOR DISPLACEMENTS ONLY, TO 1 FOR BOTH DISPLACEMENTS
C AND STRESSES, TO 2 FOR STRESSES ONLY.
C HB EQUALS H/R.
C CKR EQUALS KR
C CKP EQUALS KP
C TMB EQUALS TEMPERATURE MEAN BAR
C THB EQUALS TEMPERATURE FIRST MOMENT BAR
C PB EQUALS P BAR (TANGENTIAL PRESSURE)
C QPB EQUALS Q BAR (TRANSVERSE PRESSURE)
C WP EQUALS W BAR
C WBD EQUALS W BAR DOT (VELOCITY)
C VB EQUALS V BAR
C VBD EQUALS V BAR DOT (VELOCITY)
C CHIB EQUALS CHI BAR
C QB EQUALS Q BAR
C EPPB EQUALS EPSILON PHI BAR
C EPTB EQUALS EPSILON THETA BAR
C FKPB EQUALS KAPPA PHI BAR
C FKTB EQUALS KAPPA THETA BAR
C FNPB EQUALS N PHI BAR
C FNTB EQUALS N THETA BAR
C FMPB EQUALS M PHI BAR
C FMTB EQUALS M THETA BAR
C WA EQUALS W BAR NEXT TO APEX
C VA EQUALS V BAR AT A STATTON I=NV.
C CHOOSE N GREATER THAN OR EQUAL TO  $(1.2 \cdot PO / \sqrt{HB}) / 2$ 
C CHOOSE NV ABOUT N/2.
      DIMENSION PB(50), QPB(50), TMB(50), THB(50)
      DIMENSION TMP(50,5), STGB(5)
      DIMENSION CT1(50), CT2(50)
      DIMENSION WB(50), WBD(50), VB(50), VBD(50), CHIB(50)
      DIMENSION QB(50), FNTB(50), FNPB(50), FMPB(50), FMTB(50)
      DIMENSION WA(3500), VA(3500)
C GEOMETRIC, MATERIAL AND CONTROL DATA ENTERED HERE.
      READ(5,24) PO, HB, PP, CKR, CKP
      READ(5,24) TREF, ALFA
      READ(5,25) NBC, N, NV, MMAX, IDEC, IPRNT
24 FORMAT( )
25 FORMAT(6I10)
      L=N-1
      AN=N
      DP=2.0*PO/(2.0*AN-1.0)
      DT=0.5*DP*DP
      S1R=1.0-0.5*CKR
      S1P=1.0-0.5*CKP
      S2R=1.0+0.5*CKR
      S2P=1.0+0.5*CKP
C PRESSURE, TEMPERATURE DATA ENTERED HERE.
C TEMPERATURE INTEGRALS EVALUATED ASSUMING TEMPERATURES DEFINED AT
C FIVE EQUALLY SPACED POINTS THRU THICKNESS, NOT INCLUDING SURFACE POINTS.
C J=1,5 REFER TO POINTS NEAREST INNER, OUTER SURFACE RESPECTIVELY.
      READ(5,24) (QPB(I), PB(I), I=1,N)
      DO 20 I=1,N
      READ(5,24) (TMP(I,J), J=1,5)
      TMB(I)=(1.0*PR)*ALFA*(-TREF+1275.0*TMP(I,1)+100.0*TMP(I,2)+402.0
1*TMP(I,3)+100.0*TMP(I,4)+275.0*TMP(I,5))/1152.0/HB

```

NWC TP 5785

```

      THB(I)=(1.0*PR)*ALFA*(-11.0*TMP(I,1)-2.0*TMP(I,2)+2.0*TMP(I,4)
      1+11.0*TMP(I,5))/(9.6*HB*HB)
20 CONTINUE
      WRITE(6,21) PG,PR,CKR,CKP
      WRITE(6,22) NBC,N,NV,MMAX,HB
21 FORMAT(1H,'PO=',E11.5,2X,'PR=',E11.5,2X,'KR=',E11.5,2X,
      1'KP=',F11.5)
22 FORMAT(1H,'NBC=',I1,2X,'N=',I2,2X,'NV=',I2,2X,'MMAX=',I4,2X,
      1'HB=',F11.5)
      WRITE(6,23) TREF,ALFA
23 FORMAT(1H,'TREF=',E11.5,2X,'ALFA=',E11.5)
      WRITE(6,40)
40 FORMAT(///,5X,'TEMPERATURE DISTRIBUTION'//)
      WRITE(6,35)
      DO 42 I=1,N
      WRITE(6,41) I,(TMP(I,J),J=1,5)
42 CONTINUE
41 FORMAT(1H,'I2,2X,5(E11.5,2X)')
      WRITE(6,43)
43 FORMAT(///,5X,'SURFACE LOADING AND TEMPERATURE INTEGRALS'//)
      WRITE(6,44)
44 FORMAT(2X,'I',9X,'GPB',9X,'PB',9X,'TMB',9X,'THB'//)
      DO 46 I=1,N
      WRITE(6,45) I,GPB(I),PB(I),TMB(I),THB(I)
45 FORMAT(1H,'I2,2X,4(E11.5,2X)')
46 CONTINUE
C SET COTANGENT FUNCTIONS
      CT2(1)=COS(DP/2.0)/SIN(DP/2.0)
      DO 1 I=2,N
      FI=I
      CT1(I)=COS((FI-1.0)*DP)/SIN((FI-1.0)*DP)
      CT2(I)=COS((FI-0.5)*DP)/SIN((FI-0.5)*DP)
      1 CONTINUE
C SET TIME TO ZERO
      M=1
C SET INITIAL DISPLACEMENT, VELOCITIES TO ZERO
      DO 2 I=1,N
      WB(I)=0.0
      WBD(I)=0.0
      VP(I)=0.0
      VDD(I)=0.0
      2 CONTINUE
      WA(1)=0.0
      VA(1)=0.0
C SET APEX SYMMETRY, TANGENTIAL DISPLACEMENT BOUNDARY CONDITIONS.
      CHIB(1)=0.0
      QB(1)=0.0
      VB(N+1)=0.0
C DISPLACEMENTS COMPLETE FOR FIRST TIME STEP
C COMPUTE STRAINS, ROTATIONS, STRESS RESULTANTS FOR TIME STEP
      3 DO 4 I=2,N
      CHIB(I)=(WB(I)-WB(I-1))/DP-VB(I)
      4 CONTINUE
      DO 5 I=1,L
      EPPB=W2(I)+(VB(I+1)-VB(I))/DP
      EPTB=WB(I)+0.5*(VB(I+1)+VB(I))*CT2(I)
      FKPB=(CHIB(I+1)-CHIB(I))/DP
      FKTB=0.5*(CHIB(I+1)+CHIB(I))*CT2(I)
      FNPB(I)=EPPB+PR*EPTB-TMB(I)
      FNTB(I)=EPTB+PR*EPPB-TMB(I)
      FMPB(I)=FKPB+PR*FKTB+THB(I)
      FMTB(I)=FKTB+PR*FKPB+THB(I)
      5 CONTINUE

```

```

C SET CONDITIONS AT I=N.
  FPPB=WR(N)*(VB(N+1)-VB(N))/DP
  EPTB=WR(N)+0.5*(VB(N+1)+VB(N))*CT2(N)
  FNPB(N)=FPPB+PR*EPTB-TMB(N)
  FNTB(N)=EPTB+PR*FPPB-TMB(N)
  IF(NBC-1) 100,200,200
100 FKPB=-2.0*CHIB(N)/DP
  FMPB(N)=FKPB+THB(N)
  FMTB(N)=PR*FKPB+THB(N)
  GO TO 300
200 FMPB(N)=0.0
  CHIP(N+1)=(CHIB(N)*(1.0-0.5*PR*DP*CT2(N))-THB(N)*DP)/
  1(1.0+0.5*PR*DP*CT2(N))
  FKPB=(CHIB(N+1)-CHIB(N))/DP
  FKTB=0.5*(CHIB(N+1)+CHIB(N))*CT2(N)
  FMTB(N)=FKTB+PR*FKPB+THB(N)
300 DO 6 I=2,N
  QB(I)=(FMPB(I)-FMPB(I-1))/DP+0.5*(FMPB(I)-FMTB(I)+FMPB(I-1)
  1-FMTB(I-1))*CT1(I)
  6 CONTINUE
C STRAINS,ROTATIONS,STRESS RESULTANTS COMPLETED FOR THIS TIME STEP
C COMPUTE VELOCITIES FOR NEXT HALF TIME STEP
DO 7 I=2,N
  VBD(I)=VDB(I)*S1P/S2P*(DT/S2P)*(PB(I)+((FMPB(I)-FMPB(I-1))/DP
  1+0.5*(FNPB(I)-FNTB(I)+FNPB(I-1)-FNTB(I-1))*CT1(I)
  2-HB*HB*QB(I)/12.0)/(1.0-PR*PR))
  7 CONTINUE
  DO 8 I=1,L
  WBD(I)=WBD(I)*S1R/S2R*(DT/S2R)*(QB(I)-(FNPB(I)+FNTB(I)+
  1HB*HB*((QB(I+1)-QB(I))/DP+0.5*(QB(I+1)+QB(I))*CT2(I))/12.0
  2)/(1.0-PR*PR))
  8 CONTINUE
  IF(NBC-1) 320,320,310
310 QB(N+1)=-QB(N)
  WBD(N)=WBD(N)*S1R/S2R*(DT/S2R)*(QB(N)-(FNPB(N)+FNTB(N)+
  1HB*HB*((QB(N+1)-QB(N))/DP+0.5*(QB(N+1)+QB(N))*CT2(N))/12.0
  2)/(1.0-PR*PR))
320 M=M+1
C COMPUTE DISPLACEMENTS FOR NEXT WHOLE TIME STEP
  WP(1)=WP(1)+DT*WBD(1)
  WA(M)=WB(1)
  DO 9 I=2,L
  WR(I)=WP(I)+DT*WBD(I)
  VR(I)=VB(I)+DT*VBD(I)
  9 CONTINUE
  VB(N)=VB(N)+DT*VBD(N)
  VR(N+1)=-VR(N)
  VA(M)=VR(NV)
  IF(NBC-1) 340,340,330
330 WB(N)=WP(N)+DT*WBD(N)
340 IF(M-MMAX) 3,3,10
  10 IF(IPRNT-1) 11,11,14
  11 WRITE(6,16)
  16 FORMAT(//,2X,'DISPLACEMENTS VS. ITERATION INDEX')
  DO 13 J=10,MMAX,IDECL
  WRITE(6,12) J,WA(J),J,VA(J)
  12 FORMAT(1H,'WA(',I4,')=',E11.5,2X,'VA(',I4,')=',E11.5)
  13 CONTINUE
  IF(IPRNT-1) 15,14,14
  14 WRITE(6,30)
  30 FORMAT(//,2X,'SOLUTION IN DIMENSIONLESS VARIABLES')
  WRITE(6,31)

```

NWC TP 5785

```

31 FORMAT(2X,'I',RX,'WB',8X,'VB',8X,'NPHI-BAR',4X,'NTHETA-BAR',4X,
1'MPHI-BAR',4X,'MTHETA-BAR'/)
DO 32 I=1,N
WRITE(6,33) I,WB(I),VB(I),FNPB(I),FNTB(I),FMPB(I),FMTB(I)
33 FORMAT(1H ,I2,2X,6(E11.5,2X))
32 CONTINUE
WRITE(6,34)
34 FORMAT(//,2X,'MERIDIONAL DIMENSIONLESS STRESS THRU THICKNESS'/)
WRITE(6,35)
35 FORMAT(2X,'ZETB',2X,'-0.4',10X,'-0.2',10X,'0.0',10X,'0.2',10X,
1'0.4'/)
DO 37 I=1,N
DO 36 J=1,5
AJ=J
ZETB=-0.6+0.2*AJ
SIGB(J)=HB*(FNPB(I)-ZETB*HB*(FMPB(I)-THB(I))*TMB(I))/(1.0-PR*PR)
1-ALFA*(TMP(I,J)-TREF)/(1.0-PR)
36 CONTINUE
WRITE(6,41) I,(SIGB(J),J=1,5)
37 CONTINUE
15 STOP
END

```

INITIAL DISTRIBUTION

5 Naval Air Systems Command

AIR-320 (1)

AIR-320B (2)

AIR-50174 (2)

3 Naval Sea Systems Command

SEA-035 (1)

SEA-09G32 (2)

1 Naval Postgraduate School, Monterey

1 Naval Research Laboratory

1 Naval Surface Weapons Center, White Oak

12 Defense Documentation Center